



Caravel meshes: A new geometrical strategy to rationalize curved envelopes

Xavier Tellier, Cyril Douthe, Laurent Hauswirth, Olivier Baverel

► To cite this version:

Xavier Tellier, Cyril Douthe, Laurent Hauswirth, Olivier Baverel. Caravel meshes: A new geometrical strategy to rationalize curved envelopes. Structures, 2020, 28, pp.1210-1228. 10.1016/j.istruc.2020.09.033 . hal-03174597

HAL Id: hal-03174597

<https://enpc.hal.science/hal-03174597>

Submitted on 19 Mar 2021

HAL is a multi-disciplinary open access archive for the deposit and dissemination of scientific research documents, whether they are published or not. The documents may come from teaching and research institutions in France or abroad, or from public or private research centers.

L'archive ouverte pluridisciplinaire **HAL**, est destinée au dépôt et à la diffusion de documents scientifiques de niveau recherche, publiés ou non, émanant des établissements d'enseignement et de recherche français ou étrangers, des laboratoires publics ou privés.

This is a post-print of :

Tellier, X., Douthe, C., Hauswirth, L., & Baverel, O. (2020, December). Caravel meshes: A new geometrical strategy to rationalize curved envelopes. *Structures* (Vol. 28, pp. 1210-1228). Elsevier.

Caravel meshes: a new geometrical strategy to rationalize curved envelopes

Xavier TELLIER* ^{a b}, Cyril DOUTHE^a, Laurent HAUSWIRTH^b, Olivier BAVEREL^{a c}

* ^a Laboratoire Navier UMR8205, Ecole des Ponts, IFSTTAR, CNRS
77455 Champs-sur-Marne - MLV Cedex 2
xavier.tellier@enpc.fr

^b Université Paris-Est, Laboratoire d'Analyse et de Mathématiques Appliquées, UMR8050

^c GSA / ENS Architecture Grenoble

Abstract

Curved structural envelopes have been popular in architecture in the past decades. Their main limitation is their high cost, which is due in particular to the manufacturing complexity induced by curvature. This article introduces Caravel meshes, a new family of meshes that offers geometrical properties allowing a significant reduction of fabrication complexity. In particular, for gridshells, the most complicated fabrication aspect is usually the connection between the structural elements – beams and panels. In Caravel meshes, all these connections are rationalized. Beams are connected to panels without kinks, beams are connected top each other with repetitive which are also free of geometrical torsion. We show that a great variety of mesh combinatorics is possible with these properties. We study in particular quadrangular and hexagonal patterns. In each case, we estimate the possible shapes using differential geometry. We show that hexagonal Caravel meshes offer a significant design freedom, such that other geometrical properties simplifying fabrication can be obtained, such as edge offsets. Finally, we show that Caravel meshes offer many new ways to design curved structural systems, in which beams and panels may work together mechanically. We highlight one application for the fast prototyping of curved surfaces.

Keywords: *architectural geometry, gridshells, fabrication-aware design, curved structures, node repetition, torsion-free nodes, edge offset meshes, sandwich panels*



Figure 1: A timber gridshell at Ecole des Ponts, in which many of the properties of Caravel meshes are used to simplify fabrication. In particular, only two types of nodes are used throughout the structure, and beams are cut perpendicularly to the web, which can be done with good precision using low-tech equipment (©Stefano Borghi)

1 INTRODUCTION

Curved building envelopes have gained in popularity in the past decade. Many iconic complex doubly-curved facades have been erected, such as the Foundation Vuitton in Paris, or the Graz Art museum. Beyond its architectural potential, curvature may also allow for a significant reduction of material use and environmental impact: the theoretical optimal shape of a building envelope with respect to its mechanical performance is never flat, but doubly curved. However, curvature tends to increase drastically the cost of a building envelope, because non-standard complex elements have to be fabricated. The field of architectural geometry, also referred to as fabrication-aware design or envelope rationalization, has recently emerged to tackle this challenge (Pottmann *et al.* 2015). This field address points that are

trivial when designing a planar façade or roof, but become much more complex when considering a curved envelope. Topics include for example: how to clad a surface with planar panels? How to design a multi-layer structural system with simple connection details? How to avoid that all the constitutive elements are different?

This article introduces a new rationalization strategy for curved envelopes. It is based on *Caravel meshes*, a new geometrical mesh structure with properties which may simplify manufacturing at multiple levels. Caravel meshes are especially suited for gridshells, i.e. curved grids of beams that act structurally as shells. They are particularly adapted for ones clad with metal panels or ETFE cushions, because faces of Caravel meshes are not planar. They also allow panels and beams to work structurally together by simplifying the detailing of their connections. Other applications include the fast prototyping of curved geometries (Figure 31), and the design of curved sandwich panel structures.

Many patterns are compatible with the properties of Caravel meshes. These properties are summarized for both quadrangular and hexagonal Caravel meshes in Figure 2, they are the following:

- Caravel meshes constitute reference wireframes for gridshells with no geometrical torsion at nodes: mid planes of beams meet on a common axis;
- These beams can be clad by folded panels such that there is no kink angle between the beam top surface and the panels (Figure 3). This property simplifies significantly the connection between panels and beams. Panels may not be planar, but folded along diagonals. This is a common solution in opaque facades (Figure 4);
- Only two types of standard nodes may be used throughout the structure. For this purpose, nodes are split in two families:
 - Planar nodes, with varying in-plane angles between beams, but null vertical angles
 - 3D nodes, with varying vertical angles, but constant in-plane angles.

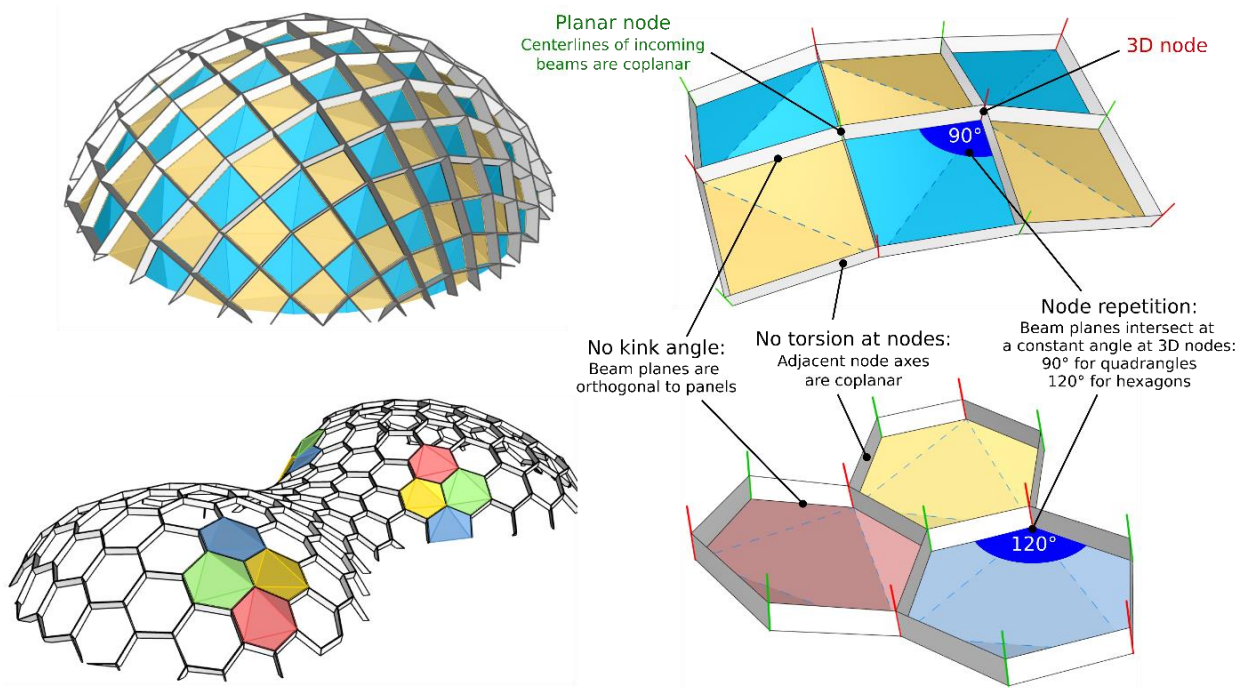


Figure 2: A quadrangular and a hexagonal Caravel mesh and their local properties. These properties are purely geometrical and aim at simplifying as much as possible the manufacturing of a curved structure while still offering a significant design freedom.

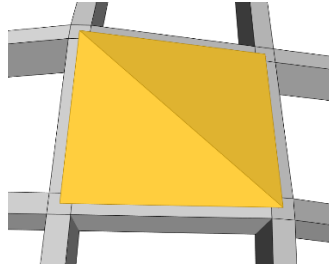


Figure 3: A panel with a diagonal fold without kink angle : panels lie flat on the top surfaces of beams. This property significantly simplifies the beam-panel connection

Considering these constructive properties, the first question that arises is: What shapes and patterns do they allow? This article focuses on this question, and also discusses potential methods to generate Caravel meshes. We do not discuss their mechanics, we rather remain focused on manufacturing aspects, which can be expressed in purely geometrical terms. Let us just mention that structural efficiency can be accounted for in a project at an early design phase by choosing an efficient surface within the design space of Caravel meshes, such as a funicular surface.



Figure 4: Diagonal folds is a common solution on opaque on façades. Left: EAVT in Marne-la-Vallée. Middle: Hamburg Poppenbüttel Bus Terminal (© www.archimages.de). Right: Rhike Park Music Theater (© Aslan Juan)

Paper overview

We start by reviewing, in section 2, the constructive properties addressed in the present paper and the associated literature. The geometry of Caravel meshes is then presented in section 3. They have an uncommon geometrical structures, with two different types of nodes, and two different types of edges. We show that a wide variety of patterns is compatible. In section 4, we focus on the simplest pattern: quadrangular Caravel meshes. We show by an asymptotic analysis based on differential geometry that they are quite constrained formally. For that reason, we turn to hexagonal Caravel meshes in section 5. The same asymptotic analysis shows that they can approximate arbitrary smooth surfaces, and thus offer an interesting design freedom. In section 6, we use the large size of their design space to introduce another geometrical property with many benefits in terms of manufacturing: edge offset. Finally, in section 7, we present structural applications of Caravel meshes. Their potential is illustrated by the construction of two full-scale pavilions: one in timber (Figure 1), and one in aluminum (Figure 30).

Preliminary remarks:

- In this article, when using the word *gridshell*, we are not talking about *elastic* gridshells, in which initially straight beams are elastically bent into shapes. We consider gridshells realized from straight beams, in which curvature is concentrated at nodes.
- By *mesh*, we refer to a set of vertices (points) connected by straight edges and faces – these faces being not necessarily planar.
- A core of the contribution is the derivation of possible shapes using differential geometry. However, the key demonstrations are postponed to the appendices for clarity.
- Numerical generation of hexagonal Caravel meshes is mentioned, but will be further detailed in future publications.

2 LITERATURE REVIEW

In this section, we review the geometrical properties that will be used in this article. Each of these properties result in a specific simplification of the fabrication.

Kink angle between panels and beams

In curved envelopes built with straight beams, there is usually a kink angle between cladding panels and support beams, as shown in Figure 5. This kink angle can make the detailing of the beam-panel connection quite complex, especially if the ratio of the panel width over the surface curvature radius is high (Figure 5, right), i.e. if the surface is coarsely discretized. In a glazed structure, a low kink angle can be accommodated by the elasticity of the EPDM joints, which are necessary for the water tightness. If the kink angle is too high, costly profiles need to be used. In an opaque façade, the kink angle is harder to deal with. In particular, it prevents the panels from acting as structural elements, unless a complex machining of the beams is performed, like in the Hybrid Shell-Nexorade Pavilion (Douthé *et al.* 2018). Solutions to cover a curved envelope without kink angle were explored in (Tellier, Baverel, *et al.* 2018).

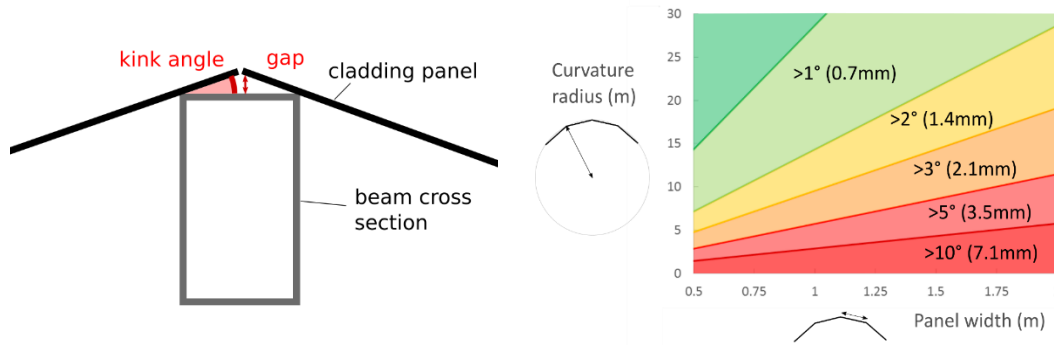


Figure 5: Kink angle between a cladding panel and a beam and corresponding gap. Right: value of the angle and gap as a function of panel width and curvature radius of surface. The gap is given for a 80mm wide beam.

Node torsion

In a gridshell, nodes are often the costliest element. Their fabrication is greatly complexified if the planes of symmetry of the incoming beams do not meet on a common axis. The node is then said to have geometrical torsion. Figure 6 compares a node with torsion in the gridshell MyZeil designed by SBP (Knippers and Helbig 2009) and an ideal torsion-free node. Problems with torsions are highly increased for beams with a high section. Torsion-free nodes are therefore particularly interesting when a gridshell has to withstand high bending moments. This typically happens when the supports cannot withstand lateral loads, and therefore membrane action is limited. Common examples are gridshells covering existing atriums, for which the walls were not designed to withstand strong out-of-plane forces. The gridshell shown in Figure 28 rests on columns and has the same limitation. The solutions to avoid torsion that are proposed in the literature generally consist in aligning edges with principal curvature directions. These are the only directions along which a surface normal does not undergo torsion (do Carmo 1976). Notable examples are circular meshes, conical meshes (Liu *et al.* 2006), and edge offset meshes (Pottmann *et al.* 2007) meshes.

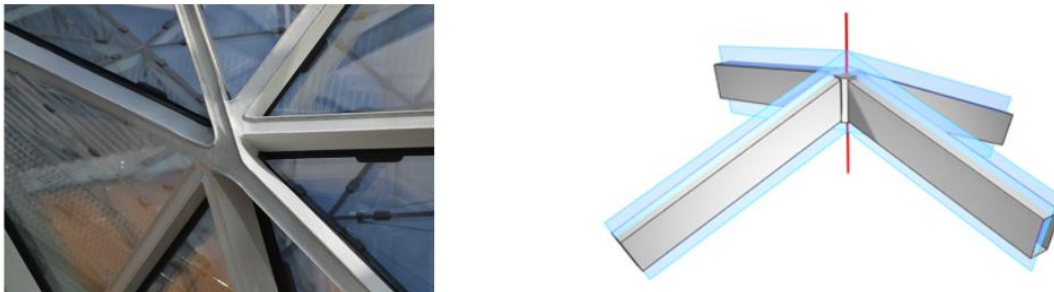


Figure 6: Left: The geometrical torsion of this node results in the need of costly and time-consuming site welding (picture: R. Mesnil). Right: Node without torsion

Edge offset

Gridshells are usually built with sections of constant heights. To insure proper connection with cladding elements, it is desirable that the centerlines of the upper flanges are aligned. This results in a kink at soffit, as showed in Figure 7. This

kink is unaesthetic, but also introduces force eccentricities at the nodes, as the beam centerlines do not meet at a common point. A consequence of such an imperfection is the likely reduction of the buckling capacity of the gridshell. Kinks also prevents from putting panels at both top and bottoms of nodes, for example when using sandwich panels. This problem is solved if nodes are *perfect*: torsion-free node for which all the incoming beams at a node have the same vertical angle. If all nodes are perfect, the mesh has a so-called edge-offset, a notion introduced in (Pottmann et al. 2007). Methods to design particular meshes with edge offsets were proposed in (Mesnil et al. 2015; Tellier, Hauswirth, et al. 2018).

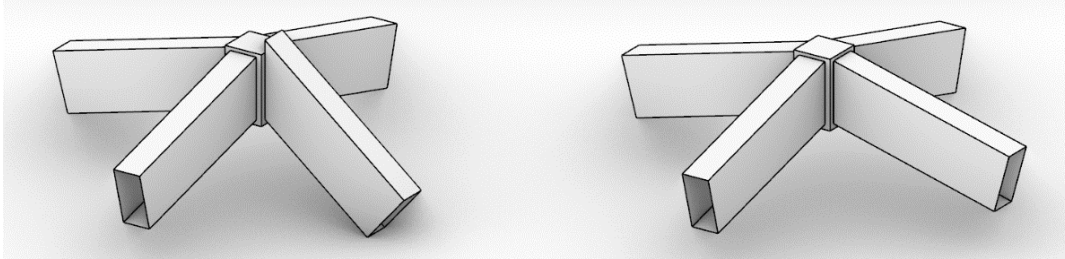


Figure 7: Alignment of soffits usually result in a kink at the node top. This is not the case in an edge offset mesh, in which all nodes are “perfect” (right)

Node repetition

Generally, in a curved envelope, each element is unique. This variation of geometry makes fabrication, structural analysis and site planning much more complex – even though fabrication complexity can be alleviated by CNC or robotic fabrication.

As nodes are the costliest elements, having a repetition of node geometry on a curved structure is of particular interest. To study node repetition, the geometry of a node needs first to be clearly described. (Stephan et al. 2004) propose to assign a reference axis to each node, which defines a reference plane normal to this axis. The geometry of each incoming beam at the node can then be described with three angles, as illustrated in Figure 8:

- A vertical angle, between the beam and the reference plane;
- A horizontal angle between beams, which is projected in the reference plane;
- A torsion angle, between the plane of symmetry of the beam and the node axis.

(Schling 2018) identified three main strategies to obtain a repetition of nodes:

i/ Make all angles identical.

This strategy works well with continuous curved beams (Bo et al. 2011; Tellier, Douthe, et al. 2019). In this paper, special attention is paid to the panel-beam connection, which leads us to focus on gridshell with straight bars which are interrupted at connection nodes. In that case, node repetition is extremely constraining on the shapes and patterns. To obtain interesting shapes, more than one type of node must be used. Few surfaces are known to work, an example being surfaces of revolution: nodes may be identical along a parallel. Identical nodes can be conserved by applying parallel transformations to these surfaces (Mesnil et al. 2015).

ii/ Use assembly tolerances so that identical nodes can accommodate slightly different angles.

This approach is implicit in most methods attempting to obtain node repetition by geometrical optimization, such as Pauly.

iii/ Design nodes such that they can accommodate variation of one of the three angles, for example with hinges.

This solution was for example used by SBP for the gridshell of the Neckarsulm swimming pool (1988), in which only one standard hinged node is used. We will use this last strategy in Caravel meshes.

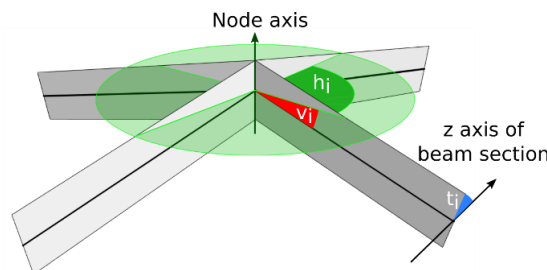


Figure 8: Description of the geometry of a gridshell node using a reference axis and its orthogonal plane

3 CARAVEL MESHES

3.1 Folded panels without kink-angle

As will be detailed in section 3.2, a key property of Caravel meshes is that they can be covered with folded panels without kink angle between beam and panels (Figure 3). We start by studying the geometrical implications of this property, which are somehow unusual.

3.1.1 Geometrical structure

Envelopes covered with folded panels without kink angle can be geometrically described by two meshes, as shown in Figure 9 (in which panels are shown in yellow and grey):

- A *structural mesh*, which represents the top centerline of support beams. This mesh also corresponds to the edges of the panels.
- A *fold mesh* (dashed), which corresponds to all the fold lines. Each node of this mesh has to correspond with one node of the structural mesh. Faces of this mesh are planar.

As seen in Figure 9, a node of the structural mesh may or may not be a node of the fold mesh. In the second case, the node is necessarily planar, i.e. all incident beam axes are coplanar. The fabrication of such nodes is significantly simpler than for that of a spatial node. Nodes of the structure can therefore be divided into two categories: *planar nodes* and *3D nodes*.

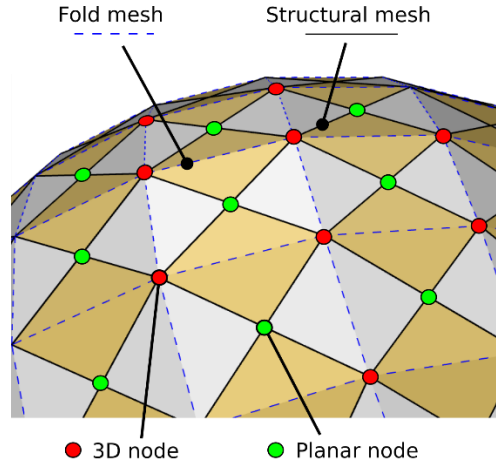


Figure 9: Fold mesh and structural mesh

Both meshes play an important role in the aesthetic of an envelope. The structural mesh defines the patterning of the surface, how it is divided into panels. The fold mesh divides the surface into planar faces. Each of these faces has a different angle in space, and will appear to a viewer with a different luminosity.

3.1.2 Topology

The topological relation of fold and structural meshes can be formalized using the theory of graphs. A graph is set of vertices linked by edges. The topology of a manifold mesh can be described by a simple planar graph, i.e. a graph that can be drawn on a plane without intersection of edges, and such that no more than one edge link two vertices. The faces correspond to the domains enclosed by edges. We propose to name a graph that is compatible with the fold mesh/structural mesh structure a *Caravel graph*, defined as follows:

Definition: A Caravel graph is a simple planar graph that fulfills the following properties:

- Vertices are bicolored: green (labeled “planar nodes”) and red (labeled “3D nodes”). Adjacent nodes may have the same color, so the graph does not need not be “2-colorable”.
- Edges are bicolored: dashed blue (folds) and black (beams).
- Each fold starts and ends at a 3D node. A node is labelled planar if and only if it has no incident fold.
- At least two folds and two beams meet at a 3D node (except on the boundary).

Condition iv. is due to the facts that we do not allow a lone cantilevered beam in the mesh, and that at least two fold lines must meet for the node not to be planar. Despite condition i, a Caravel graph need not be 2-colorable: two adjacent nodes can have the same color. Figure 10 shows two examples of Caravel graphs. The graph of the structural mesh can be retrieved from a caravel graph by taking the beams and all the nodes. Similarly, the fold mesh is retrieved by taking the folds and the 3D nodes.

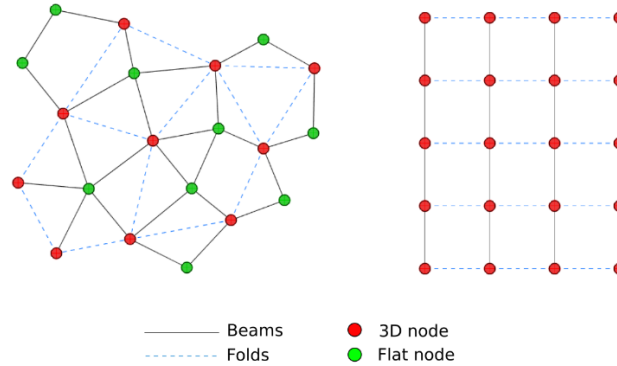


Figure 10: Caravel graphs

The structural and the fold meshes are not dual of each other. In particular, one cannot in general swap the colors of the edges and nodes, as the condition of having two folds and two beams meeting at a 3D node gets violated.

3.1.3 Possible periodic patterns

There is a great variety of mesh topologies satisfying the Caravel graph properties. In particular, many patterns with periodic combinatorics are possible. The *semi-regular* tessellations of the plane (also called Archimedean tilings) provide a good basis to generate new combinations of fold and structural meshes. Semi-regular tessellations are planar periodic patterns obtained by assembling regular polygons (e.g. equilateral triangle, square, regular pentagon...) such that at each vertex, the same types and numbers of polygons meet, in the same order. These tessellations are described by a sequence of digits that correspond to the number of edges of each polygon around a node. For example, a Kagome pattern is called (3,6,3,6), because at each vertex, two regular triangles and hexagons meet alternatively. From a semi-regular tessellation, one can build a dual tiling by connecting the centers of all the pairs of adjacent polygons.

Figure 11 shows twelve combinations of structural and fold meshes, most of them generated from semi-regular tessellations or from their duals. Colors correspond to faces of the structural mesh, and therefore to panels.

- In pattern (a) (the same as in Figure 2), both fold mesh and structural mesh are quadrangular. There is one fold in each face of the structural mesh.
- Patterns (b) to (d) show other ways to arrange quadrangular panels with one fold. Each of them gives a very different fold mesh and structural mesh combinatorics. For example, in pattern (c), the structural mesh is the dual of the Archimedean tiling (3,3,3,3,6), and the fold mesh is a Kagome mesh.
- In pattern (e), the structural mesh is hexagonal. This type of mesh can be realized by tri-folded hexagonal panels. This type will be the object of sections 5 and 6. The fold mesh is a triangular mesh.
- Pattern (f) is derived from a (3,4,6,4) fold mesh. The structural mesh is composed of quadrangles with one fold and hexagons with three folds.
- In patterns (g) and (h), some faces of the structural mesh are not folded. These can be used to insert panels made of materials that cannot be folded, such as glass. Pattern (g) is based on a structural mesh composed of hexagons and quadrangles, while pattern (h) is derived from an octo-quad fold mesh.
- Patterns (i) and (j) shows patterns with quadrangular panels that have respectively two and four folds. In pattern (j), the 3D nodes have only two incoming beams, which correspond to a kink in a beam.
- Pattern (k) is based on a Penrose pattern, a non-periodic pattern with a rotation symmetry of order five.
- Pattern (l) uses a dodecahedron as a fold mesh. Its flat nodes are 5-valent, while its 3D nodes are only 3-valent.

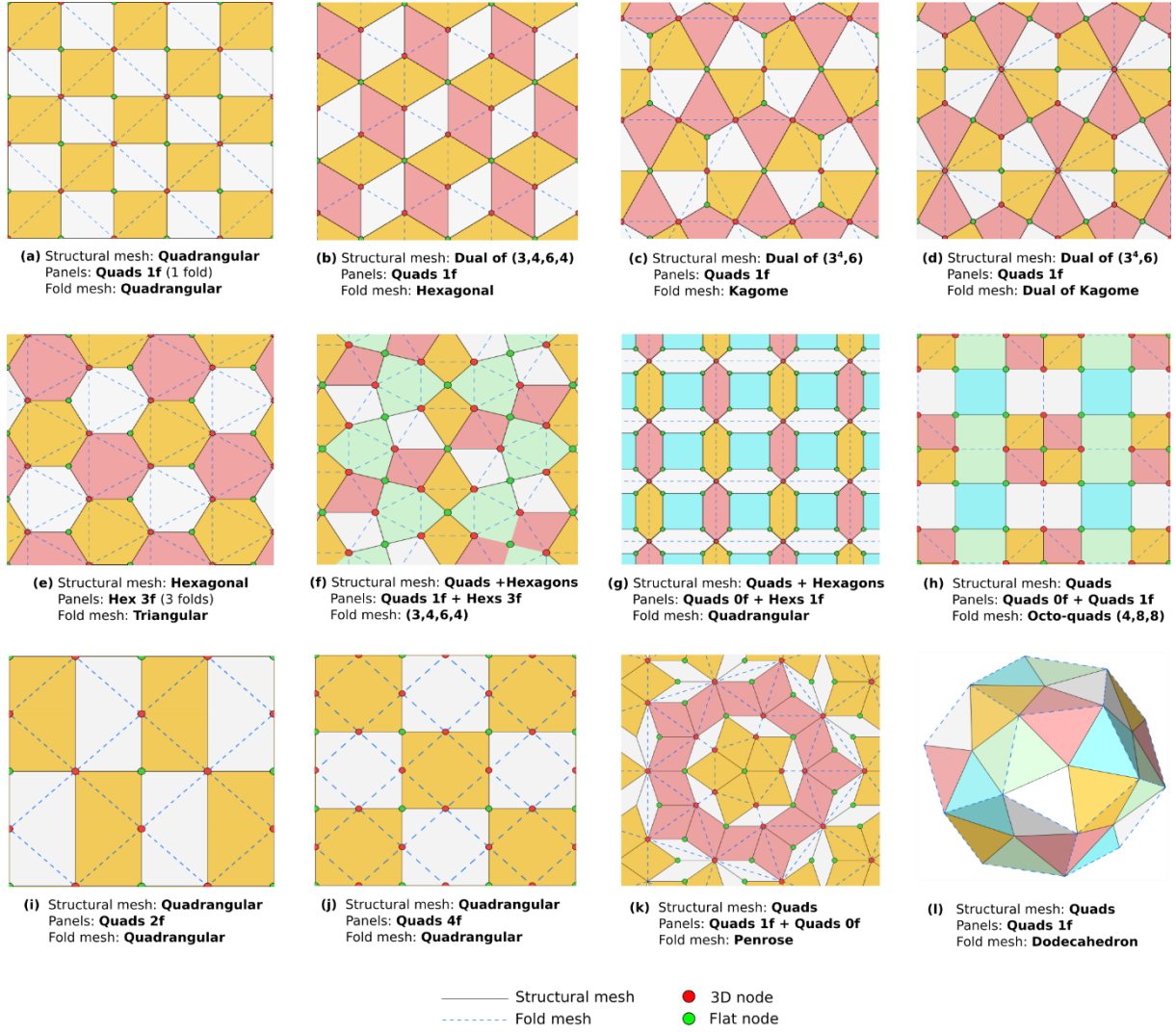


Figure 11: A great variety of patterns is compatible with Caravel meshes

3.1.4 Generation

Even though this is outside the scope of Caravel meshes, let us mention that the generation of meshes with folded panels and no-kink angles is relatively straight forward. These can be generated in two steps. The first one is the construction of a fold mesh with planar faces (see for example (Jiang *et al.* 2015), (Glymph *et al.* 2004), (Wang and Liu 2009) or (Vaxman and Ben-chen 2015) for the patterns above). The second step consists in drawing a structural mesh on the faces. For example, Figure 12 shows a realization of pattern (c) where a Kagome mesh has been generated by the method described in (Mesnil *et al.* 2017). Mechanically, the structural mesh can be efficiently decomposed into a principal load carrying system made of a triangular network of near planar arches, and a secondary system to support the panels, forming a hexagonal pattern. The resulting structure combines elegantly (in our humble opinion) four different types of meshes: Kagome (planar faces), triangular (principal structure), hexagonal (secondary structure), and dual (3⁴,6) (folded panels).

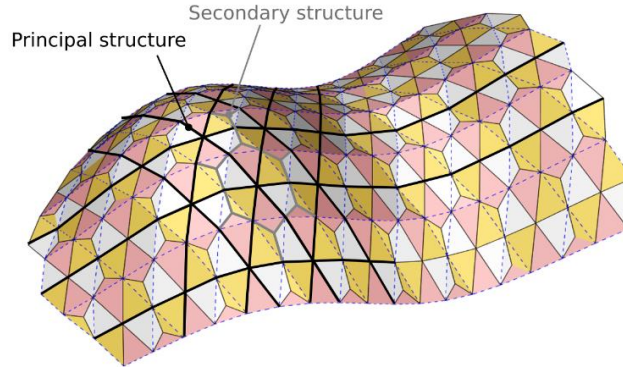


Figure 12: A geometric realization of the pattern (c) of Figure 11

3.2 Caravel meshes

The constructive properties of Caravel meshes that are detailed in section 1 can be expressed in a purely geometrical fashion. The property of having no kink angle was just discussed in section 3.1, it can now be combined with the properties of having a torsion-free support structure and repetitive nodes (Figure 2):

Definition: a *Caravel mesh* is a mesh with Caravel graph combinatorics and axes at each vertex such that:

- (a) The axes of two adjacent nodes are coplanar - their common plane corresponds to the median plane of the beam;
- (b) At “planar nodes”, the incoming beams are coplanar;
- (c) Axes at “planar nodes” are perpendicular to the plane defined by the adjacent edges.
- (d) Node repetition: horizontal angles between beams at 3D nodes is constant

Properties (b) and (c) guarantee a null kink angle, property (a) guarantees no torsion, while properties (a), (b) and (d) insure together a new node repetition strategy, discussed more in detail in the next sections. We insist on the fact that this definition is based only on manufacturing considerations, and unrelated to mechanics or a given material.

The name Caravel is chosen as an invitation to explore new structural systems using *meshes with CoplanAR fAcE and VERtEx normaLs*. This name highlights the interplay of vertex normals and face normals of the fold mesh. Previous literature on torsion-free structures has focused on the geometric torsion between node normals combined with a constraint on face planarity (for example (Pottmann and Wallner 2007), (Liu et al. 2006)), the study of these meshes constitutes therefore a new topic and poses new geometric challenges.

Amongst all the combinatorics showed in Figure 11, we will study in more details patterns (a) in section 4, as it is simple and efficient mechanically. We will also study pattern (e) in sections 5 and 6 because of the greater design freedom it offers.

4 QUADRANGULAR CARAVEL MESHES

Quadrangular Caravel meshes, as the one showed in Figure 2, appear to be the most simple pattern out of the ones showed in Figure 11. Furthermore, the continuity of beam orientation gives them good mechanical performance. We hence study in detail their possible shapes in this section, and propose a generation method. We discover that the design space is limited to a specific family of synclastic surfaces.

4.1 Possible shapes

4.1.1 Asymptotic behavior

In this subsection, we consider how the geometric structure of quadrangular Caravel meshes behave in the asymptotic case, i.e. in the case where a smooth surface is approximated by a series of meshes with smaller and smaller face size (Figure 13). We show in particular the following results:

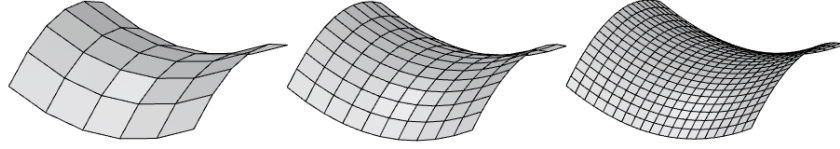


Figure 13: Approximating a surface with meshes of decreasing face size

Asymptotic behavior:

- A surface approximated by quadrangular Caravel meshes is necessarily synclastic.
- Beams tend to align with principal curvature directions of the surface.
- The aspect ratio of the faces of the mesh is prescribed by the ratio of the principal curvatures. More precisely, edges tend towards a surface parametrization by principal curvature lines $(u, v) \mapsto x(u, v)$ of the surface such that at any point (Figure 14):

$$\frac{\|x_u\|}{\|x_v\|} = \sqrt{\frac{k_2}{k_1}} \quad (1)$$

- Not any synclastic surface can be approximated. Indeed, a principal parametrization fulfilling equation (1) cannot be found on an arbitrary surface. Surfaces of revolution belong to this family, but the space of possible shapes is unknown at the moment.

The proof is given in appendix A. Even though these result pertain to Caravel meshes with infinitely small edges, they influence strongly the geometry of a quadrangular mesh in general. For example, the fact that negative curvature is impossible will be proven for meshes in the next sub-section.

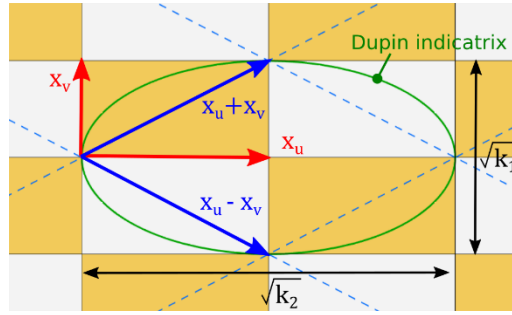


Figure 14: Quadrangular Caravel mesh: In the asymptotic case, a face of the fold mesh is a diamond inscribed in a homothetic image of the Dupin indicatrix

Note:

The fact that the aspect ratio of the faces of the fold mesh is constrained by the principal curvatures ratio can be more intuitively understood using the concept of Dupin indicatrix (which is recalled in appendix B). In the asymptotic case:

- A face is congruent to the neighboring faces (Wang and Liu 2009). As a consequence, faces must have central symmetry.
- The fold mesh is a conjugate net, its faces are therefore inscribed in a Dupin indicatrix.
- The diagonals of the fold mesh are aligned with curvature directions, i.e. with the main axes of the indicatrix.

The only solution to this set of constraints is for the faces of the fold mesh to be diamonds inscribed in the Dupin indicatrix in Figure 14. As such, their shape is entirely prescribed by the ratio of the major and minor axes of the indicatrix, which are proportional to the square roots of the principal curvatures.

4.1.2 Impossibility of anticlastic meshes

The fact that anticlastic surfaces (i.e. with negative Gaussian curvature (saddle-shaped) at each point) are impossible can be more intuitively understood on a mesh than on a smooth surface. In Figure 15, we consider an anticlastic 3D node and the four adjacent faces of the fold mesh. One planar node is constructed on each face (at an arbitrary location). We then construct in blue the planes defined by the node axes of planar nodes and the beam axes adjacent to the 3D node. The intersection lines of pairs of planes are drawn in blue. We observe that the planes do not intersect on a common line (the blue lines do not coincide) whatever the position of the planar nodes on the faces. Hence, a torsion-free support structure

cannot be found. A consequence is that perfect quadrangular Caravel meshes can only be used for structures like domes or “blobs”, in which the Gaussian curvature is usually everywhere positive.

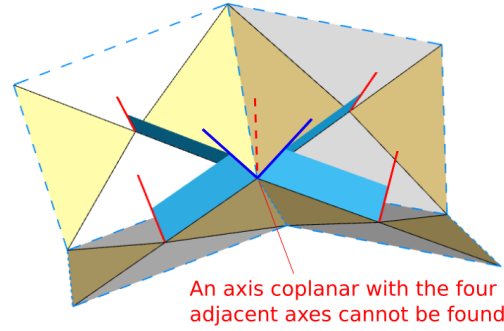


Figure 15: A quadrangular Caravel mesh cannot be anticlastic.

4.1.3 Node repetition

As mentioned in section 2, the geometry of a node can be described by three sets of angles: vertical, horizontal and torsion angles of each incoming beam. For the planar nodes of Caravel meshes, the vertical angle (as shown in Figure 8) is zero. This property can simplify significantly their fabrication. In the asymptotic analysis of section 4.1.1 and appendix A, we considered surface parametrizations in which iso-lines cross everywhere at 90° . In a mesh, it is impossible to have 90° between edges at all nodes of a mesh (except in trivial cases like cylindrical or planar meshes). However, it is possible to have a horizontal 90° angle between beams at 3D nodes only – and not at planar nodes. The geodesic curvature (k_g) of a mesh polyline is then concentrated in the planar nodes, while the normal curvature (k_n) is concentrated at 3D nodes – an example is shown in Figure 16. Table 1 summarizes the repetition properties, and studies the comparison with circular and conical meshes, the most popular torsion-free quad structures.

Planar Quad meshes		Circular/conical mesh	Quad Caravel mesh	
Nodes			2D nodes	3D nodes
Horizontal angle	Variable	Variable	Variable	90°
Vertical angle	Variable	Variable	0°	Variable
Torsion angle	Variable	0°	0°	0°
Faces			Fold mesh	Structural mesh
Planarity	Planar	Planar	Planar	Non-planar
Beam-panel assembly				
Beam-panel angle	Variable	Variable		0°

Table 1: Comparison of repetitivity between quad Caravel mesh other torsion-free quad mesh structures

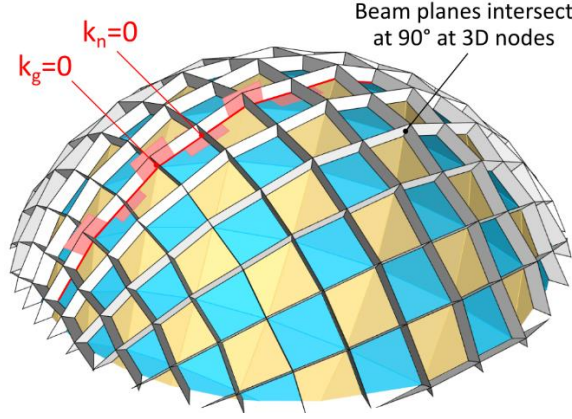


Figure 16: A quad Caravel mesh of revolution. The normal and geodesic curvature of beams are respectively concentrated at 3D nodes and planar nodes.

4.1.4 Introducing mesh singularities

Quadrangular Caravel meshes have nodes of valence four and faces with four edges. However, singularities can be introduced, in which one node is not four-valent, or one face is not quadrangular. Singularities are topologically necessary for a pattern to cover a closed surface. They also allow to introduce significant curvature with limited distortion of the pattern. Singularities can be concisely described by the notion of *index*. Intuitively (see Figure 17, right), the index can be calculated as follows: looping around a singularity in the positive direction, a vector field aligned with one family of edges does not align with its starting orientation after a loop. The number of turns it did is called the index. A positive index most often occurs in synclastic surfaces, while negative indexes occur generally in anticlastic surfaces. See (Takens 1974) for a thorough treatment, or (Petit 1985) for an entertaining introduction.

For quadrangular patterns, the index is always a multiple of $\frac{1}{4}$. Singularities of index $k/4$ with $k > 0$ are shown in Figure 17. Because of the two-colorability constraints on the nodes, only indexes $+\frac{1}{2}$ and $+1$ are possible for Caravel meshes. This constraint is also imposed by the fact that the mesh needs to be aligned with curvature lines: Singularities of curvature line networks (umbilics) always have an index which is a multiple of $\frac{1}{2}$ (Gutierrez and Sotomayor 1998). For example, the mesh of revolution in Figure 18 would require a singularity $+1$ to close the middle hole.

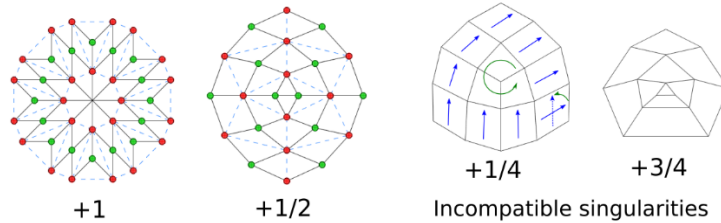


Figure 17: Singularities of a quadrangular Caravel meshes may only have an index $+1$ or $+1/2$

4.2 Generation of meshes with symmetry of revolution

As discussed in section 4.1, the space of possible surfaces is unknown. However, synclastic surfaces of revolution work. To construct such meshes, one only needs to generate a proper strip of quads along a meridian. The degrees of freedom are shown in Figure 18, and can be chosen in this order: the angular width of the strip Θ , the slope of the meridian at the base α , the lengths $l_1, l_2 \dots l_n$ of the exterior edges of the strip. The choice of these length will automatically define the curvature of the meridian. This method can be tedious for a designer because the degrees of freedom are not intuitive to control. However, it is a simple way to obtain the Caravel properties exactly. The 90° angle at 3D node can be obtained by this method by choosing proper values of $l_2, l_4 \dots l_{2k}$. For sake of concision, we will omit further details.

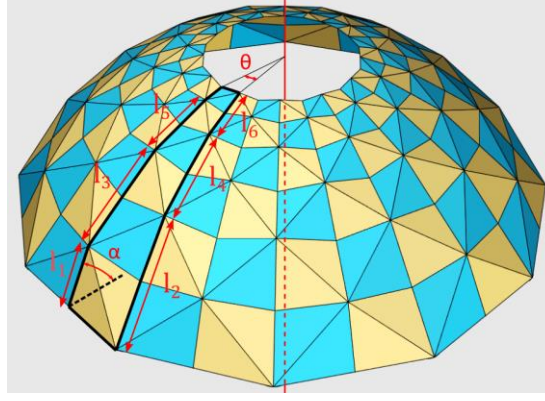


Figure 18: Degrees of freedom to generate a quad Caravel mesh of revolution

5 HEXAGONAL CARAVEL MESHES

The major limitation of Caravel quad meshes is their design freedom: they do not allow negative curvature, and the spacing between beams is imposed by the ratio of the principal curvatures. Thanks to the lower valence of the nodes, hexagonal Caravel meshes (pattern (e) in Figure 11, see also Figure 2) do not suffer from this limitation, and their geometry is much less constrained. Furthermore, contrary to planar hexagonal meshes, Caravel hexagon meshes can cover surfaces with negative Gaussian curvature with convex hexagons, whereas planar hexagons necessarily take the shape of a bow-tie (Figure 19).

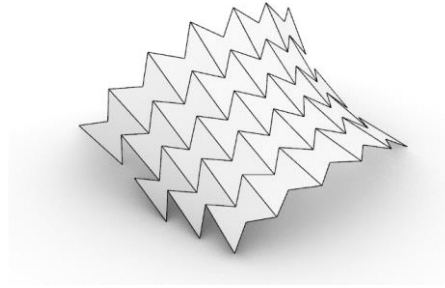


Figure 19: Constraining a gridshell with hexagonal pattern to have planar faces results in bow-tie shaped faces on anticlastic (saddle) surfaces. Caravel hexagonal meshes do not suffer from this limitation

5.1 Possible shapes

5.1.1 Without node repetition

We start by considering hexagonal meshes which fulfill properties (a), (b) and (c) of Caravel meshes (section 3.2), but not (d). We start by this case as it occurs naturally first in our demonstration flow. We observe that the asymptotic behavior of this type of mesh is much less constraining than for quadrangular Caravel meshes (section 4.1):

Asymptotic behavior:

Any smooth surface can be approximated by a hexagonal mesh with properties (a) to (c) of Caravel meshes. The hexagonal pattern aligns with conjugate nets: referring to Figure 20, there exist a direction i for which vectors e_i and S_i are conjugate.

Conjugate nets can be seen as a discrete equivalent of quadrangular meshes with planar lines. We are not going to discuss them more in depth in this article, but the reader can find a theoretical introduction in (do Carmo 1976), and the design of conjugate nets on a surface is discussed in (Zdravcevic et al. 2010). However, let us just mention that they let a significant patterning freedom on synclastic surfaces, and that principal curvature nets are a particular conjugate net in which lines cross at 90° .

The proof of this asymptotic behavior is given in appendix B.

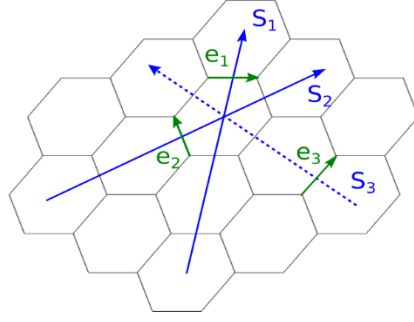


Figure 20: Directions of edges and short diagonals of a hexagonal mesh

5.1.2 Hexagonal Caravel meshes

Let us now consider all the Caravel properties together, (a) to (d). Similarly to quad Caravel meshes, repetition can be introduced in the 3D nodes (property (d) of section 3.2) by setting the horizontal angles between beams at 120° for each 3D node. This results in the following asymptotic behavior:

Asymptotic behavior:

Any smooth surface can be approximated by a hexagonal Caravel mesh. Hexagons are then aligned with principal curvature directions. This means that one family of edge, and one short diagonal is aligned with principal curvature directions, as shown in Figure 21. Umbilics on the surface might lead to discontinuities of the Caravel pattern.

The proof is given in appendix C. We observe that hexagonal Caravel meshes offer a great design freedom, as they can approximate any surface. The orientation of the patterns is however restrained for a given surface. The umbilics of the surface must correspond to singularities in the pattern, a point that we discuss in the upcoming subsection.

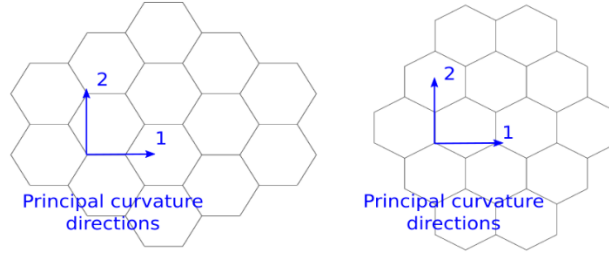


Figure 21: Hex mesh aligned with principal curvature directions on a surface. Two orientations are possible.

5.1.3 Singularities

As for the case of quad Caravel meshes discussed in section 4.1.4, not all types of singularity are possible in a hexagonal mesh. As shown in Figure 22, singularities in hexagonal meshes have an index $k/6$ ($k \in \mathbb{Z}$). In order to keep the two-colorability of the nodes in the pattern, the index must be $k/3$ – otherwise, a rupture of the pattern would be visible along a line, as visible on the singularity $+1/6$. Four configurations of interest are shown in Figure 22. If the 120° node repetition is strongly enforced, the net must be aligned with principal curvature directions. As the index of umbilics is $k/2$ ($k \in \mathbb{Z}$), only indexes that are multiple of both $1/2$ and $1/3$ are possible, i.e. indexes $+1$ and -1 . These two types of singularity require a high variation of the metrics of the pattern.

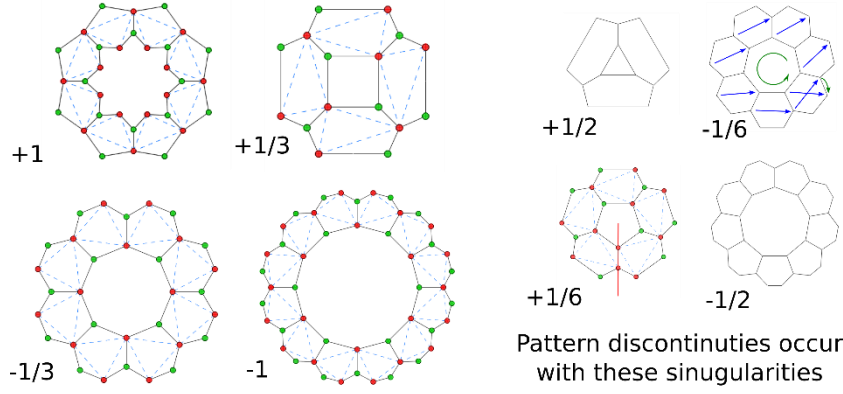


Figure 22: Allowable singularities of hexagonal Caravel meshes and their index. Only singularities of index +1 and -1 are compatible with the 120° node repetition strategy. Patterns on the right result in pattern discontinuities.

5.2 Generation

Here, we discuss briefly how hexagonal Caravel meshes can be generated from a smooth surface by optimization. This topic will be addressed more in detail in further work. It was in particular implemented for the design of IASS HeX-Mesh pavilion (Tellier et al. 2020). The following construction steps can be used:

- i. Generate a hexagonal network aligned with principal curvature directions;
- ii. Construct a staggered grid using Fermat points, as explained in Appendix C (Figure 36);
- iii. Optimize the geometry so that it satisfies all the properties of a Caravel mesh, using for example the projection-based optimization framework described in (Deng et al. 2015).

If the target surface has umbilics, the pattern may have discontinuities. It is therefore preferable to use surfaces that do not have umbilics, for example Monge surfaces or surfaces with planar curvature lines in one or two directions (Mesnil et al. 2018; Tellier, Douthe, et al. 2019).

6 HEXAGONAL CARAVEL MESHES WITH EDGE OFFSET

As discussed in the introduction, having a mesh with an edge offset offers remarkable fabrication possibilities. Due to the large design freedom offered by hexagonal Caravel meshes, it is possible to obtain edge offset on the top of properties (a) to (d) (section 3.2). Resulting meshes constitute a subset of hexagonal Caravel meshes.

6.1 Possible shapes

Asymptotic behavior

- A synclastic surface approximated by a Caravel mesh with edge offset must admit a parametrization by principal curvature lines such that:

$$\frac{\|x_u\|}{\|x_v\|} = \frac{k_2}{k_1} \quad (2)$$

Regular hexagons (i.e. with an aspect ratio close to 1) are obtained only on spherical surfaces.

- An anticlastic surface approximated by a Caravel mesh with edge offset must admit a parametrization:

$$\frac{\|x_u\|}{\|x_v\|} = -\frac{1}{2\sqrt{3}} \frac{k_2}{k_1}$$

Regular hexagons are obtained if the surface is Linear Weingarten, fulfilling:

$$2\sqrt{3}k_1 + k_2 = 0$$

Equation (2) can be directly compared with equation (1). Similarly to quad meshes, the aspect ratio of the hexagons (the ratio $\|x_u\|/\|x_v\|$) is imposed by the curvature of S . However, this aspect ratio is now proportional to k_2/k_1 instead of $\sqrt{k_2/k_1}$. Therefore, a much higher variation of aspect ratio is required to mesh non-spherical surfaces. If one wants to design a grid with an aspect ratio close to 1 ($\|x_u\| \simeq \|x_v\|$), one is restricted to near-spherical surfaces ($k_2 \simeq k_1$).

6.1.1 Proof

We do not postpone the proof to the appendix, because the proposed generation method in section 6.2 is based on this proof.

We start by remarking that the 2D nodes are already perfect, as the vertical angle is 0° for each beam, so edge offset adds a constraint only to the 3D nodes. Making a 3D node perfect imposes a strong symmetry on the node: the horizontal angle between beams is constant (120°), and the norm of the vertical angle is also constant (the sign of the vertical angle may vary). Examples of 3D nodes with edge offset and 120° in plane angles are shown in Figure 23, both with positive and negative curvature.

These properties strongly constrain the Gauss mesh. Indeed, the Gauss map of a 3D node verifies the following properties:

- Because of the 120° horizontal angle and the torsion-free property, the spherical angles between the Gauss map of the edges is also 120° ;
- Since the vertical angles are equal, the distance between the Gauss image of a 3D node and Gauss images of the adjacent 2D nodes is constant.

Combining these two properties together, the Gauss images of three 2D nodes adjacent to a given 3D nodes form an equilateral triangle if Gaussian curvature is positive (triangle $N_1N_2N_3$ in Figure 23, middle bottom). If Gaussian curvature is negative, they form an isosceles triangle, in which the height at the apex is half of the length of the two equal edges – the 3D node is then outside of this triangle (Figure 23, right bottom). We remark that, because faces of Caravel meshes are not planar, the Gauss image is not a Koebe polyhedron, contrary to the previous studies of edge offset meshes in the literature (for example (Pottmann et al. 2010)). Gauss map for surfaces with positive and negative curvature are shown in Figure 24.

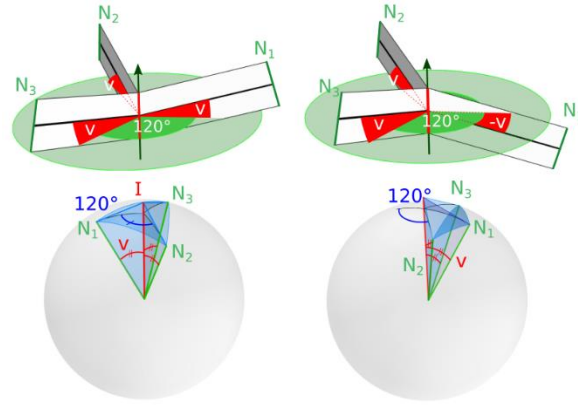


Figure 23: Left node: Non perfect node. Middle and right: Perfect nodes with 120° horizontal angle, with positive (middle) and negative (right) curvature. Bottom: corresponding Gauss map.

Let us now use these discrete considerations to study the asymptotic behavior.

Synclastic surfaces

If curvature is positive, the fact that the Gauss mesh is built from equilateral triangles (shown in green) imposes that the sphere is conformally parametrized:

$$n_u \cdot n_v = 0 ; \|n_u\| = \|n_v\| \quad (3)$$

Curvature in directions u and v are then given by:

$$k_1 = \frac{\|n_u\|}{\|x_u\|} ; k_2 = \frac{\|n_v\|}{\|x_v\|}$$

We obtain:

$$\frac{\|x_u\|}{\|x_v\|} = \frac{k_2}{k_1}$$

Equations (3) imply that we can find a parametrization by curvature lines on S for which the Gauss map is conformal. For this parametrization to exist, the surface has to belong to the family of so-called “L-isothermic surfaces” (Blascke 1929; Pottmann et al. 2007), so meshing an arbitrary surface is not possible.

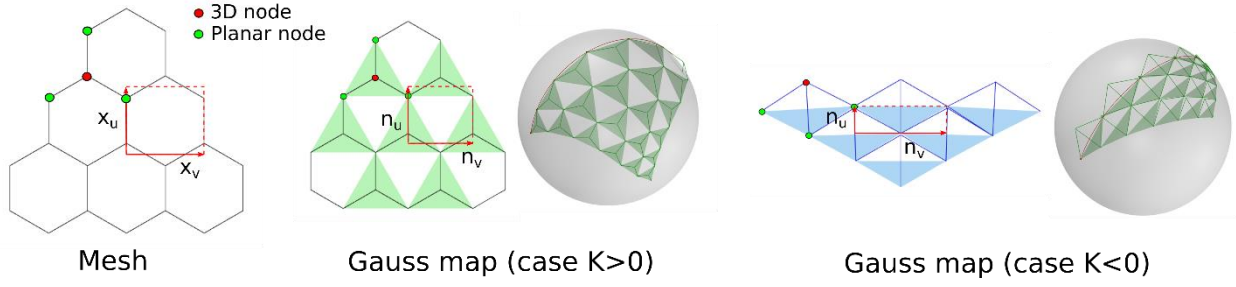


Figure 24: Gauss map of hexagonal Caravel mesh with edge offset

Anticlastic surfaces

If Gaussian curvature is negative, we have $k_2 < 0 < k_1$. Basic trigonometry yields (Figure 24, right):

$$\|n_u\| = \frac{1}{2\sqrt{3}} \|n_v\|$$

Therefore:

$$\frac{\|x_u\|}{\|x_v\|} = -\frac{1}{2\sqrt{3}} \frac{k_2}{k_1}$$

To design a grid with an aspect ratio close to 1, we now need the surface to verify $k_2 \simeq -2\sqrt{3}k_1 \simeq -3.5k_1$. That is, the surface is both isothermic and close to a Weingarten surface $2\sqrt{3}k_1 + k_2 = 0$ in which the ratio of principal curvature is a constant. The generation and the interesting design potential of this family of surfaces was recently studied in (Jimenez et al. 2019).

6.2 Generation

Hexagonal Caravel meshes with edge offset cannot be generated on a random surface, and hence require a specific shape generation method. We propose here an approach similar to the construction of planar quad meshes with edge offset from a Koebe polyhedron given in (Pottmann et al. 2007): we build a surface by constructing first a Gauss map.

The Gauss map of a synclastic surface is conformal, and would be best constructed using tools from discrete differential geometry on that topic. However, things are much more complicated for a surface combining both synclastic and anticlastic portions. As illustrated in (Tellier, Hauswirth, et al. 2018), a fold appears on the Gauss map. This fold connects a portion of positive curvature with $\|n_u\| = \|n_v\|$ to a portion of negative curvature with $\|n_u\| = \frac{1}{2\sqrt{3}} \|n_v\|$. There is no existing numerical tool to handle this. We therefore propose a specific generation method.

We start by remarking that, in the case $K>0$, meshes of equilateral triangles can be controlled by the position of vertices along a line, as shown in Figure 25: If the position of the red nodes is known, the position of all the other vertices is entirely determined (for example, the position of C is entirely determined by the position of A and B). We can then build the Fermat points and obtain a hex mesh with 120° property. The same result holds if $K<0$.

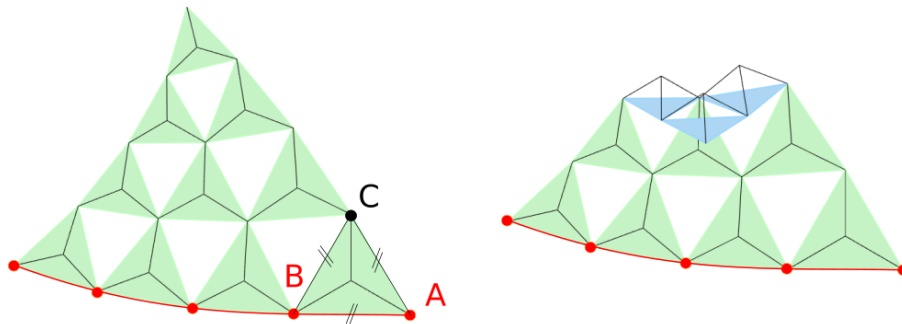


Figure 25: Construction of a valid Gauss map from a row of points (in red). Left: $K>0$ everywhere. Right: $K>0$ for the bottom two rows, $K<0$ for the top two rows (in blue).

Change of curvature sign (fold on the Gauss map) can be easily handled between two rows of hexagons. An example is shown in Figure 25, where the first two rows at the bottom have a positive curvature, while the top two rows have a negative curvature, and are therefore built downwards.

The hexagons can then be deformed by a *Combescure transform*. A Combescure transform, also called parallel transform, modifies edge lengths while keeping fixed the orientation of edges and faces. These can be controlled by the lengths of some boundary edges, as done in (Mesnil et al. 2015). The proposed degrees of freedom are shown in Figure 26.

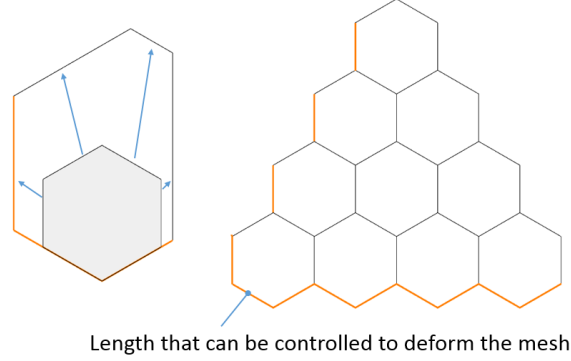


Figure 26: Deformation of the Gauss mesh by Combescure transform

We can then generate edge offset meshes with the following method:

- i. Explore meshes of equilateral triangles by drawing rows of points on the sphere, and trying out change of curvature at different rows;
- ii. Build the tangent planes to the unit sphere at the planar nodes. For each equilateral triangles, the tangent planes at the vertices intersect at a point which is aligned with the sphere center and the Fermat point of the triangle, and thus has the 120° angle between beam planes. This intersection point is therefore a planar node. We postpone the proof to the end of the section.
- iii. Deform the mesh by Combescure transform by varying the edge lengths along the boundary.

Examples of structures designed with this method are shown in Figure 27 and Figure 28. The latter one highlights how hexagonal meshes allow to cover a triangular domain with a good alignment of the pattern with the boundaries – something not allowed by quadrangular meshes.

Limitations

Some trials and errors are often needed to construct an interesting Gauss map without self-intersecting faces.

Note - Proof of the construction in step ii

Let us consider a spherical equilateral triangle $N_1N_2N_3$ (Figure 23), the tangent planes at the vertices, and the intersection point I of these three tangent planes. I is equidistant to the vertices : $IN_1 = IN_2 = IN_3$. It is therefore aligned with the sphere center and the circumcenter of the triangle. Since the triangle is equilateral, the circumcenter coincides with the Fermat center.

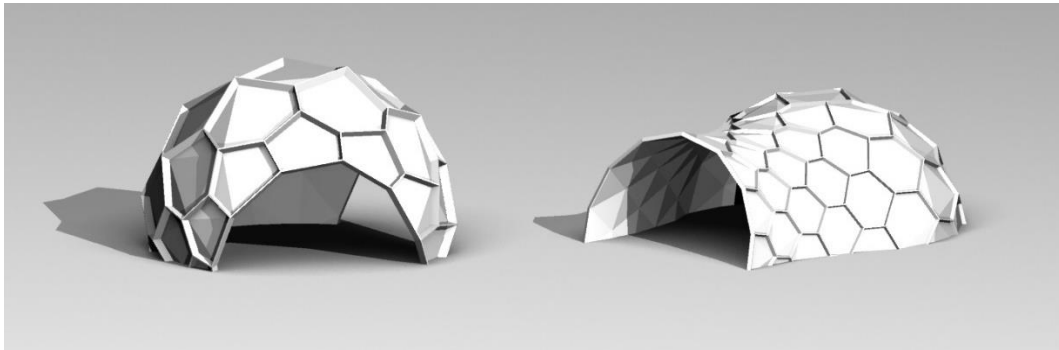


Figure 27: Structures based on hexagonal Caravel meshes with exact edge offset and node repetition

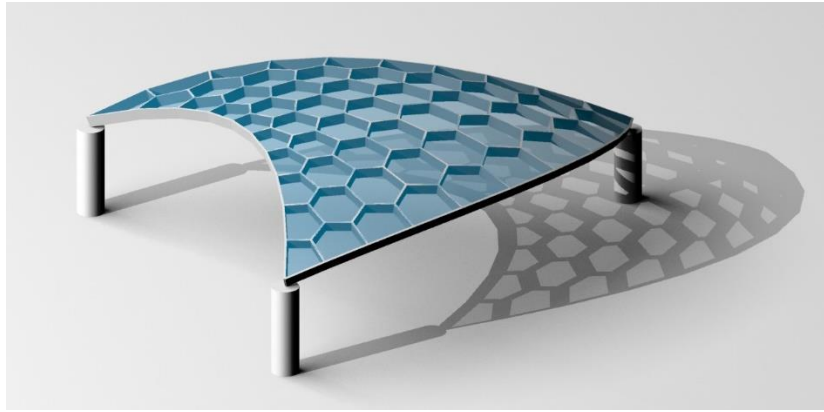


Figure 28: A shading structure based on a hexagonal Caravel mesh with only two types of nodes (planar and “120°”) and edge offset. The fact that nodes are torsion-free with edge offset allows to easily give structural height to this gridshell, thus making it resistant in bending. This structure also highlights the potential of hexagonal meshes to cover triangular surfaces with a pattern aligned with the boundaries.

7 APPLICATIONS

Properties of Caravel meshes can be used to simplify the fabrication of curved structural systems in many different ways. We will suggest here a few applications.

7.1 Structural beam-panel connection

Since panels lay flat on the top beam surface, the connection between beams and panels can be structural – for example bolted or nailed. This connection can be used to design various structural systems.

Gridshell braced by panels

Panels can be used as bracing elements for the beams. In that case, diagonal cables or moment connection are not needed anymore, thus lowering the cost of the structure.

Gridshell with beams reinforced by panels

Panels can also be used to strengthen the beams. In the pavilion showed in Figure 30, beams are made out of aluminium sheets. The panels on top and bottom restrain the beams from buckling in their weak direction and from lateral torsional buckling.

Double-layer shell

If panels are the load carrying elements, our geometry allows to connect two layers. Beams can then transfer the shear forces between the top and bottom layers, and give a significant bending strength to the shell. Hexagonal Caravel meshes with edge offset (section 6) are particularly adapted for this application, as the two layers of panels can be connected with beams of constant height (the same beam section can be used throughout the structure). These two layers of panels can form a sandwich panel.

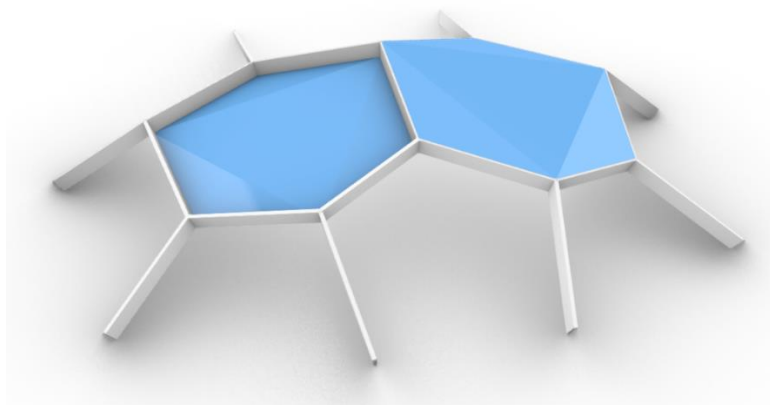


Figure 29: With edge offset, panels can be located on top and bottom of beams of constant section

7.2 Rationalization of nodes

The geometrical properties of Caravel meshes may also be used to rationalize the fabrication of the nodes of a gridshell. Figure 30 illustrates how these properties were used in the design of the HeX-Mesh pavilion, built for the 2019 IASS lightweight pavilion contest (Tellier, Zerhouni, et al. 2019). The geometry of the pavilion is based on a hexagonal Caravel mesh. The structure is composed of laser-cut aluminum sheets. One family of plates acts as beams, and is located between node axes. As plates are weak in bending, they are reinforced on their top and bottom faces by orthogonal plates. The 90° angle allows a connection by inserts and slits that can be carved by laser, as the laser cuts only at a right angle. The 120° is used to design a standard 3D node – the variations of the vertical angle at the node being accommodated by laser cutting.

The structure showed in Figure 1 is also built with only two types of nodes. The structure is composed of straight 6x14cm timber beams. The planar nodes are realized by plywood planks, screwed on top and bottom of beams. The 3D nodes are built from a timber profile with hexagonal cross-section, chopped up in 18-cm high segments. Beams are connected to the 3D nodes with 24cm-long 8mm screws. The vertical angle at 3D nodes is accommodated by sawing the beams ends with an inclined angle. The cut plane is perpendicular to the beam, this allows for a high precision even if sawing is done by hand without numerical tools.

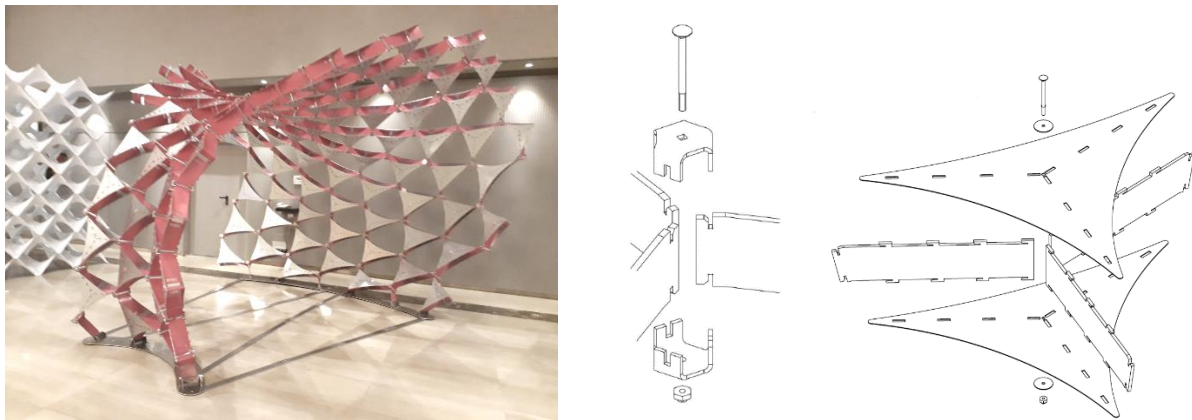


Figure 30: Pavilion rationalized by a hexagonal Caravel mesh. Details of the 3D and planar nodes.

7.3 Fast prototyping of curved surfaces

The repetition of nodes can be used to prototype quickly curved surfaces. An example is showed in Figure 31. Beams and 2D nodes are laser-cut MDF, and 3D nodes are 3D printed. All elements are clipped together. 3D nodes are the most complex elements, that is why they are 3D printed. However, as they always have the same shape (this is thanks to properties (a) and (d) of Caravel meshes (section 3.2)), they can thus be 3D printed ahead of time. The variation of the vertical angle at 3D nodes is accommodated by the laser cut of the beam ends. 2D nodes are realized by clipping planar elements (planarity is guaranteed by property (b)) on top and bottom of beams. Beams and connection plates can be clipped together as they are orthogonal (this is thanks to property (c) – a laser cutting machine can only cut at 90°).

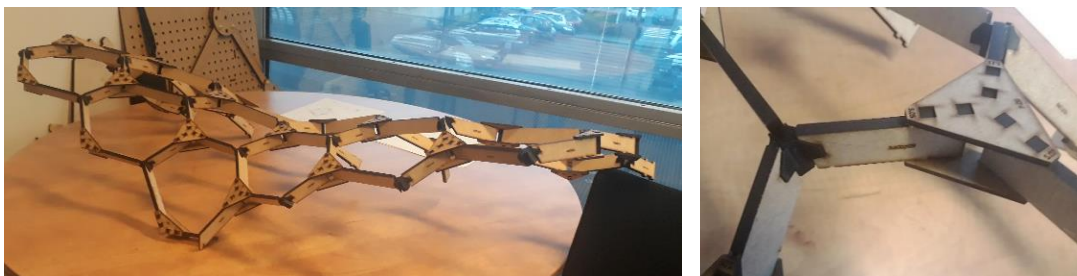


Figure 31: These mockup are realized with standard 3D printed nodes and laser-cut elements. 3D printing is time-consuming (up to 15 hours), but can be done ahead of time as nodes are identical, whatever the surface. A great variety of shapes is accessible, and production time is governed by laser cutting – which is usually done in less than 20 minutes.

7.4 Use fold mesh for paneling

The application of Caravel meshes described in section 7.1 deals with folded panels for which the boundaries coincide with the beams. However, since the fold mesh has planar faces, it can be constructed from planar panels. In that case, the torsion-free beam structure does not coincide with the panel edges anymore. An example is shown in Figure 32. This system still offers many geometric properties useful for rationalization:

- Beams are orthogonal to panels,
- 2D nodes are planar,
- 3D nodes intersect at 90°,
- No torsion at nodes.

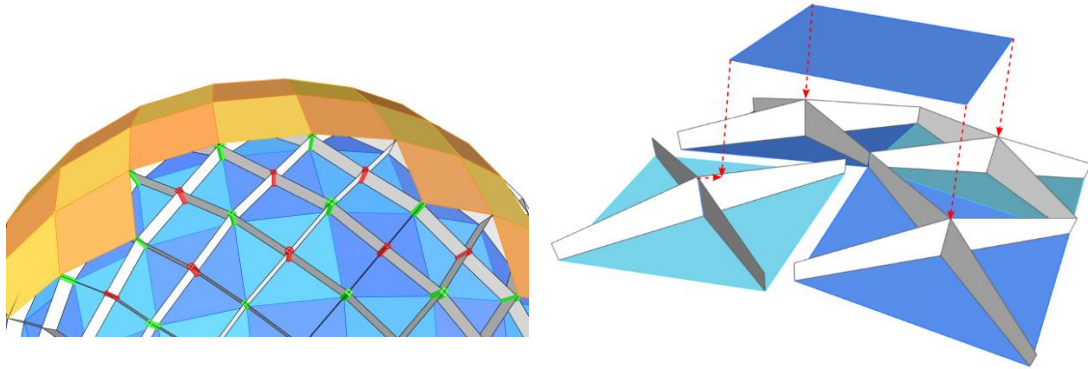


Figure 32: Alternative panelings of a quad Caravel mesh. Left: Panels aligned with the fold mesh, they are hence planar and do not require folding. Right: Staggered offset

7.5 Staggered offset

Caravel meshes are well suited for multi-layer systems thanks to the absence of torsion. Figure 32 (left) shows a structure in which two layers are arranged such that one face corresponds to one face of the offset. However, it is also possible to lay the second layer in a staggered fashion, such that one face corresponds to a node of the offset. An example is shown in Figure 32 (right). In this configuration, the grid separating the two layers of plates has tapered beams. Each node has one planar face, and one 3D face. This configuration can allow different rationalization strategies.

8 CONCLUSION

In this article, we introduced a new family of meshes, baptized Caravel meshes, aimed at making curved structures more accessible. Caravel meshes allow to design curved structural systems in which fabrication complexity may be significantly reduced. In particular, for a gridshell, there is no kink angle between beams and cladding panels, nodes are free of geometrical torsion and are repetitive. An interesting variety of patterns is compatible. We studied in particular the geometry and formal potential of quadrangular and hexagonal patterns. While quadrangular Caravel meshes are constrained to synclastic shapes, hexagonal ones offer a great design freedom, such that the additional property of edge offset can also be included. We discussed some generation methods. From a designer's perspective, their inputs are: 1/ a set of length parameters for quadrangular Caravel meshes of revolution, 2/ an arbitrary surface for hexagonal ones, and 3/ a guide curve on the unit sphere and length parameters for hexagonal meshes with edge offsets.

We also showed some of the many ways in which Caravel meshes can be used to rationalize the connections of a gridshell and to design innovative structural systems for curved envelopes – in particular by using the fact that the connection between panels and beams is perfect to make them work structurally together. Two full scale pavilions were built, with a remarkably low manufacturing complexity: all structural elements were fabricated with 3-axis cutting equipment, apart from 3D nodes, which are identical throughout the structures.

ACKNOWLEDGEMENT

The work was supported by Labex MMCD. The mockup showed in Figure 31 were realized by Juan Cruz AVELLANEDA CUFRE, Adèle GILSON, Ignacio Maria OLALQUIAGA VARELA and Piotr GALICKI during a workshop at Ecole des Ponts. We warmly thank all the people involved in the construction of the heX-Mesh and Coriolis pavilions.

REFERENCES

- Blascke, W. (1929) *Vorlesungen Über Differentialgeometrie, Vol. 3*, Springer. ed.
- Bo, P., Pottmann, H., Kilian, M., Wang, W., Wallner, J. (2011) 'Circular arc structures', *ACM Trans. Graph.*, 30(4), 101:1–101:12, available: <http://doi.acm.org/10.1145/2010324.1964996>.
- do Carmo, M.P. (1976) *Differential Geometry of Curves and Surfaces*, Prentice-Hall, Inc.
- Deng, B., Bouaziz, S., Deuss, M., Kaspar, A., Schwartzburg, Y., Pauly, M. (2015) 'Interactive design exploration for constrained meshes', *CAD Computer Aided Design*, 61, 13–23, available: <http://dx.doi.org/10.1016/j.cad.2014.01.004>.
- Douthe, C., Mesnil, R., Baverel, O., Gobin, T., Tellier, X., Ducoulombier, N., Montagne, N. (2018) 'Design and construction of a shell-nexorade hybrid timber structure', *Proceedings of the IASS Symposium 2018: Creativity in Structural Design, Boston, USA*, (July), 1–8.
- Glymph, J., Shelden, D., Ceccato, C., Mussel, J., Schober, H. (2004) 'A Parametric Strategy for Freeform Glass Structures Using Quadrilateral Planar Facets', *Automation in Construction*, 13(2), 187–202.
- Gutierrez, C., Sotomayor, J. (1998) 'Lines of curvature , umbilic points and Carathéodory conjecture Introduction', *Resenhas IME-USP*, 3(3), 291–322.
- Jiang, C., Tang, C., Vaxman, A., Wonka, P., Pottmann, H. (2015) 'Polyhedral Patterns', *ACM Transactions on Graphics (TOG)*, 34(6).
- Jimenez, M.R., Müller, C., Pottmann, H. (2019) 'Discretizations of surfaces with constant ratio of principal curvatures', *Discrete & Computational Geometry*.
- Knipppers, J., Helbig, T. (2009) 'Recent developments in the Design of Glazed Grid Shells', *International Journal of Space Structures*, 24(2), 111–126.
- Liu, Y., Pottmann, H., Wallner, J., Yang, Y.-L., Wang, W. (2006) 'Geometric modeling with conical meshes and developable surfaces', *ACM Transactions on Graphics*, 25(3), 681.
- Mesnil, R., Douthe, C., Baverel, O., Leger, B. (2017) 'Marionette Meshes : Modelling free-form architecture with planar facets', *International Journal of Space Structures*, 32(3–4), 184–198.
- Mesnil, R., Douthe, C., Baverel, O., Léger, B. (2018) 'Morphogenesis of surfaces with planar lines of curvature and application to architectural design', *Automation in Construction*, 95, 129–141.
- Mesnil, R., Douthe, C., Baverel, O., Léger, B., Caron, J.F. (2015) 'Isogonal moulding surfaces: A family of shapes for high node congruence in free-form structures', *Automation in Construction*, 59, 38–47.
- Petit, J.-P. (1985) *Le Topologicon (English Version: Topo the World)*, Belin, France.
- Pottmann, H., Eigensatz, M., Vaxman, A., Wallner, J. (2015) 'Architectural geometry', *Computers and Graphics (Pergamon)*, 47, 145–164.
- Pottmann, H., Grohs, P., Blaschitz, B. (2010) 'Edge offset meshes in Laguerre geometry', *Advances in Computational Mathematics*, 33(1), 45–73.
- Pottmann, H., Liu, Y., Wallner, J., Bobenko, A.I., Wang, W. (2007) 'Geometry of multi-layer freeform structures for architecture', *ACM Transactions on Graphics*, 26(3), 65.
- Pottmann, H., Wallner, J. (2007) 'The focal geometry of circular and conical meshes', *Advances in Computational Mathematics*, 29(3), 249–268.
- Sauer, R. (1970) *Differenzengeometrie*, Springer, Berlin.
- Schling, E. (2018) *Repetitive Structures, PhD Manuscript, TUM, Fakultät für Architektur*.
- Stephan, S., Knebel, K., Sanchez-Alvarez, J. (2004) 'Reticulated Structures On Free-Form Surfaces', *Stahlbau*, 73(April), 562–572.
- Takens, F. (1974) 'Singularities of vector fields', *Publications mathématiques de l'I.H.É.S.*, 43, 47–100, available: http://www.numdam.org/item?id=PMIHES_1974__43__47_0.
- Tellier, X., Baverel, O., Douthe, C., Hauswirth, L. (2018) 'Gridshells without kink angle between beams and cladding

panels', *Proceedings of the IASS Symposium 2018: Creativity in Structural Design, Boston, USA*.

- Tellier, X., Douthe, C., Hauswirth, L., Baverel, O. (2019) 'Surfaces with planar curvature lines: Discretization, generation and application to the rationalization of curved architectural envelopes', *Automation in Construction*, 106.
- Tellier, X., Hauswirth, L., Douthe, C., Baverel, O. (2018) 'Discrete CMC surfaces for doubly-curved building envelopes', in *Advances in Architectural Geometry*, 166–193.
- Tellier, X., Zerhouni, S., Jami, G., Le Pavec, A., Lenart, T., Lerouge, M., Leduc, N., Douthe, C., Hauswirth, L., Baverel, O. (2019) 'Hybridizing vertex and face normals to design torsion free structures : application to the X-mesh pavilion', in *Proceedings of the IASS Annual Symposium: Form & Forces, Barcelona*, 505–512.
- Tellier, X., Zerhouni, S., Jami, G., Le Pavec, A., Lenart, T., Lerouge, M., Leduc, N., Douthe, C., Hauswirth, L., Baverel, O. (2020) 'The Caravel heX-Mesh pavilion , illustration of a new strategy for gridshell rationalization', *SN Applied Sciences*, 2(781), available: <https://doi.org/10.1007/s42452-020-2561-2>.
- Vaxman, A., Ben-chen, M. (2015) *Dupin Meshing : A Parameterization Approach to Planar Hex-Dominant Meshing*, Tech. Rep. CS-2015-01, Department of Computer Science, technion-IIT.
- Wang, W., Liu, Y. (2009) 'A Note on Planar Hexagonal Meshes', in *Nonlinear Computational Geometry*, 221–233.
- Zdravce, M., Schiftner, A., Wallner, J. (2010) 'Designing Quad-Dominant Meshes with Planar Faces', in *Computer Graphics Forum*, Oxford, UK: Blackwell Publishing Ltd., 1671–1679.

APPENDIX A : ASYMPTOTIC BEHAVIOR OF QUAD CARAVEL MESHES

In this section, we prove the asymptotic behavior of quadrangular Caravel meshes given in section 4.1.1.

In the asymptotic case, properties can then be described in the setting of smooth differential geometry. On a smooth surface S , the only directions in which the surface normal does not undergo torsion are the curvature directions (do Carmo 1976). Because of the torsion-free property of the structural mesh, it necessarily tends towards a curvature line network in this asymptotic case. Let us introduce the associated parametrization by curvature lines $(u, v) \mapsto x(u, v)$. A line $x(u, v)$ with $u = \text{constant}$ or $v = \text{constant}$ is then a line of the structural mesh.

Because of the planarity constraint, the fold mesh tends in the limit case towards a conjugate net (Sauer 1970). As a result, the "diagonal directions" of the parametrization x , $x_u + x_v$ and $x_u - x_v$, must be conjugate to each other (Figure 14). Let us note dn the second fundamental form of the surface (i.e. $dn(w)$ is the vector giving the rate of change of the surface normal when we move on the surface with a velocity vector w , see (do Carmo 1976) for a thorough treatment). The conjugate condition can be written:

$$\begin{aligned} dn(x_u + x_v) \cdot (x_u - x_v) &= 0 \\ dn(x_u) \cdot x_u - dn(x_u) \cdot x_v + dn(x_v) \cdot x_u - dn(x_v) \cdot x_v &= 0 \end{aligned}$$

Since x_u and x_v are principal curvature directions, $dn(x_u) \cdot x_v = 0$ and $dn(x_v) \cdot x_u = 0$. As a result:

$$dn(x_u) \cdot x_u = dn(x_v) \cdot x_v$$

The matrix of the second fundamental form in the (u, v) plane can then be written:

$$II = \begin{bmatrix} dn(x_u) \cdot x_u & dn(x_u) \cdot x_v \\ dn(x_v) \cdot x_u & dn(x_v) \cdot x_v \end{bmatrix} = \lambda_p \begin{bmatrix} 1 & 0 \\ 0 & 1 \end{bmatrix}$$

with λ_p a real number, function of the position on the surface. Noting k_1 and k_2 the principal curvatures in the directions x_u and x_v (i.e. $k_1 = dn(x_u) \cdot x_u / \|x_u\|^2$), the matrix of the first fundamental form is (if $k_1 \neq 0 \neq k_2$):

$$I = \begin{bmatrix} x_u \cdot x_u & x_v \cdot x_u \\ x_u \cdot x_v & x_v \cdot x_v \end{bmatrix} = \begin{bmatrix} k_1 & 0 \\ 0 & k_2 \end{bmatrix}^{-1} \lambda_p \begin{bmatrix} 1 & 0 \\ 0 & 1 \end{bmatrix} = \lambda_p \begin{bmatrix} k_1^{-1} & 0 \\ 0 & k_2^{-1} \end{bmatrix}$$

The diagonal coefficients of the first fundamental form are positive. Therefore, k_1 and k_2 must have the same sign: the Gaussian curvature $K = k_1 k_2$ is necessarily positive. This confirms the intuition showed in Figure 15. Furthermore, the ratio of the metrics $\|x_u\|$ and $\|x_v\|$ of the parametrization is imposed by the curvature of the surface:

$$\frac{\|x_u\|}{\|x_v\|} = \sqrt{\frac{k_2}{k_1}}$$

Finally, we remark that one cannot find *a priori* a parametrization fulfilling the equations $x_u \cdot x_v = 0$ and $\Pi = \lambda_P \begin{bmatrix} 1 & 0 \\ 0 & 1 \end{bmatrix}$ on an arbitrary synclastic surface. The description of the possible shapes is an open problem.

APPENDIX B : HEXAGONAL CARAVEL MESHES WITHOUT NODE REPETITION

We prove the asymptotic behavior of hexagonal meshes with properties (a), (b) and (c) of Caravel meshes. We show that we can construct a mesh with these properties at the first order from a planar hexagonal (PHex) mesh.

B.1 Preliminary: Designing a gridshell on a surface which is torsion-free at the first order

Contrary to quad meshes, hex meshes do not tend towards a surface parametrization at the limit, so we start by introducing a geometrical method to design grids on a surface which are torsion-free at the first order.

The Gauss map

Let us start by recalling some elementary concepts of surface geometry. Let us consider a point P on a smooth surface, as shown in Figure 33. The unit normal at P , called the Gauss map of P , $n(P)$, can be described by a point on the unit sphere. Considering a small displacement u on the surface, $P + u$ is at the first order included in the tangent plane at P , T_P . The variation of the normal from P to $P + u$ is at the first order a vector of the tangent plane of the sphere at $n(P)$. We identify this tangent plane to T_P . The variation of the normal at P is given by the second fundamental form of the surface. This form can be expressed as a linear map on T_P :

$$dn(u) = - \begin{bmatrix} k_1 & 0 \\ 0 & k_2 \end{bmatrix} \begin{pmatrix} u_1 \\ u_2 \end{pmatrix}$$

where $u = u_1 e_1 + u_2 e_2$ is the decomposition of u in the basis of principal curvature directions (e_1, e_2) of T_P . The second fundamental form can be interpreted as a combination of two 1D-scalings, respectively in the directions e_1 and e_2 , with factors $-k_1$ and $-k_2$.

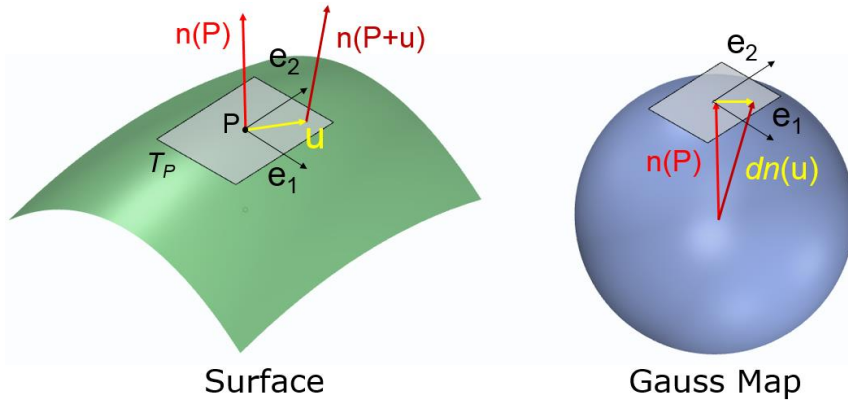


Figure 33: Gauss map of a smooth surface

First-order periodicity

All the planar patterns shown in Figure 11 are *periodic* : there exist non-collinear vectors t_1 and t_2 such that the pattern is invariant under a translation by t_1 or t_2 .

When covering an arbitrary surface with one of these patterns, they cannot be geometrically periodic anymore because of the variations of metric on the surface (the combinatorics is still periodic though). However, in the limit case where the face size is much smaller than the curvature radii of the surface and pattern, the pattern is locally periodic at the first order in the tangent plane of the surface. The Gauss map of the pattern is then also locally periodic, with period $dn(t_1)$ and $dn(t_2)$.

Torsion-free grids at first order

Let us now consider a grid of beams based on a periodic pattern in this first-order limit case. If the node axes coincide with the surface normals, the geometrical torsion can be assessed by looking at whether beams are parallel with their Gauss map. More precisely, the torsion of the surface normal along the beam is the tangent of the angle between an edge and its Gauss map. This is illustrated in Figure 34. The mesh on the top-left is aligned with curvature directions, and has therefore no torsion: $dn(t_1) \parallel t_1$. The mesh on the bottom left is not aligned with curvature direction. As a result, $(dn(t_1), t_1) = \alpha \neq 0$, and the torsion along the mesh is $\tau_g = \tan \alpha$ (expressed in rad/m). The only way to obtain a torsion-free structure is then to align all the edges with curvature directions, which is quite restrictive. This is the strategy used for quad Caravel meshes.

However, there is much more design freedom if we allow the node axes to deviate from surface normals. This is illustrated in Figure 34 (right) for an octo-quad pattern. If axes coincide with surface normals, beams of the diamonds undergo a torsion $\tan \alpha$. Now, axes can also be chosen such that beams are parallel to their Gauss map (thus yielding a torsion-free structure) *and* such that the Gauss map pattern still has periods $dn(t_1)$ and $dn(t_2)$. This is illustrated in Figure 34 at the bottom-right. The second property allows to keep the angle between the node axes and the surface normals to the first order. Without it, the axes would deviate more and more from the surface normals as we move away from P.

In order to differentiate node axes from surface normals, we will use a capital N for the former, and a lowercase n for the latter.

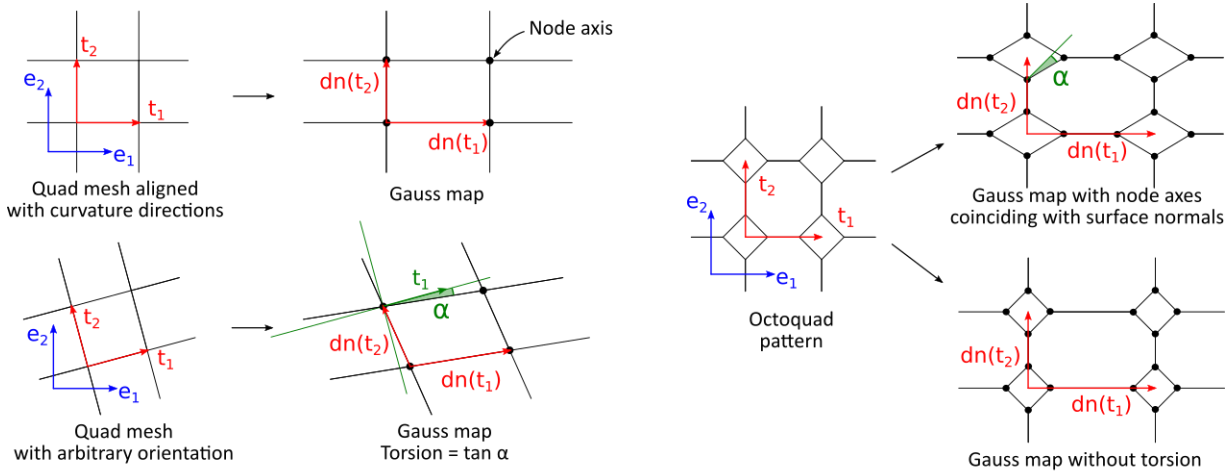


Figure 34: Understanding torsion free patterns with the Gauss map. Left: A quad pattern is torsion free only if it is aligned with principal curvature directions. Right: An octo-quad pattern can be made torsion-free even if some edges are not aligned with principal curvature direction by allowing node axes to deviate from surface normals

B.2 Construction from a PHex mesh

The strategy that we just described to generate torsion-free gridshells can be used to obtain hexagonal meshes with Caravel properties at the first-order from a mesh with planar hexagons.

Step 1: Construction of a PHex mesh

Any smooth surface can be approximated by a PHex mesh. There are locally two degrees of freedom in the orientation of a PHex hexagonal pattern (Wang and Liu 2009), for example directions S_1 and S_2 in Figure 20 (edges directions e_i are conjugate to strip directions S_i). As illustrated in, Figure 35 (left), when face size tends to zero, each hexagon tends to be planar, congruent to its neighbor, to have central symmetry and to be inscribed in a homothetic copy of the Dupin indicatrix (Wang and Liu 2009) – the Dupin indicatrix being the conic resulting from the intersection between the paraboloid and the plane $z=1$. As shown in Figure 35 (right), the surface Gauss map of the Dupin indicatrix is also a conic, with equation $\frac{x^2}{k_1} + \frac{y^2}{k_2} = 1$.

Step 2 : construction of staggered hex grid

Once a PHex mesh is drawn on the surface, the 2nd step is to build a staggered grid. Such a grid is shown in red in Figure 35. It is built by combining half of points of the PHex mesh (e.g. A,C and E) and one point inside each hexagon (e.g. P). This point is *on* the plane ACE, not on the surface – this is a second order nuance.

As will be proven in section B.3, whatever the orientations of the planar hexagons, it is possible to find center points (for example P, Q and R in Figure 35) such that all the Caravel properties (see definition in section 3.2) are fulfilled:

- (a) There exist node axes N_P, N_Q, \dots such that the grid is torsion-free (this is insured by parallelism of edges with their Gauss map, for example $PE \parallel N_P N_E$).
- (b) P, Q, R are located on the planar hexagons, and are therefore planar nodes (for example $P \in (ACE)$);
- (c) The normal at P, N_P is perpendicular to the face ACE;

A, C, E are the 3D nodes (there is no geometrical constraint associated to them).

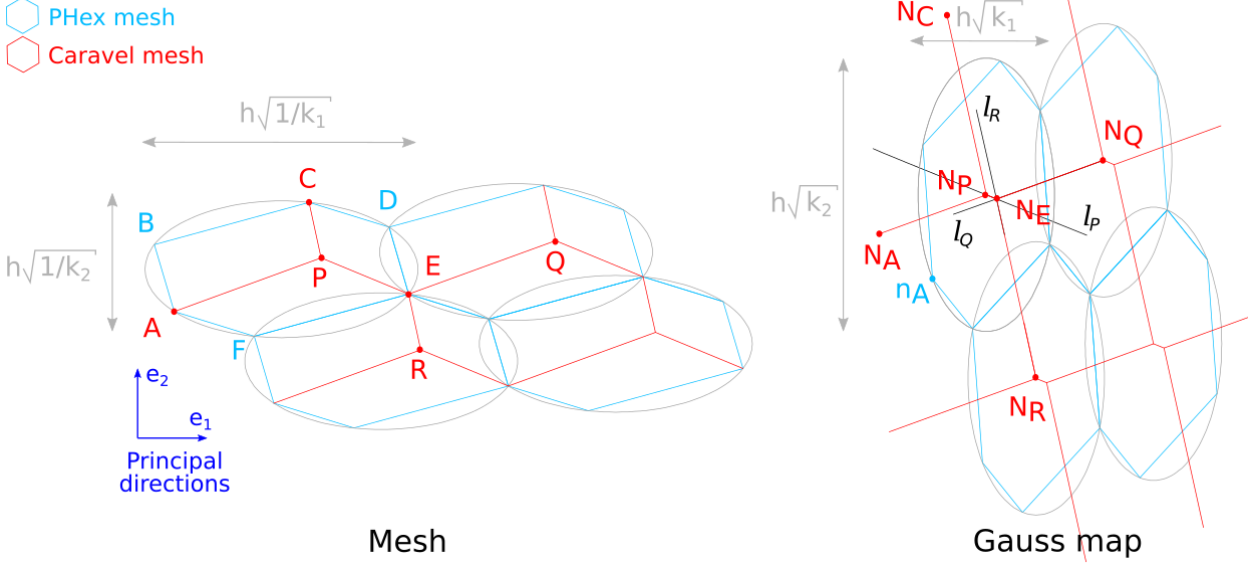


Figure 35: Asymptotic construction of a hexagonal Caravel mesh from a mesh of planar hexagons (left). Right: Gauss map

B.3 Proof of first-order constructibility

We now show that the construction of step 2 in section B.2 is possible. We refer to Figure 35.

Property (b): Planar “Planar nodes”

This property is verified by constructing points P, Q and R on the faces of the PHex mesh.

Property (c): axes at planar nodes normal to the plane of the node

Because of the central symmetry of hexagon (ABCDEF), the normal to the plane (ACE) coincides with the surface normal at the center of the indicatrix. On the Gauss map, this normal is the center of the conic. Property (c) is obtained by locating the normal N_P precisely at this center.

Property (a): torsion-free structure

Analysis of the constraint

Let us assume we have a point P fulfilling conditions (a) to (c). We recall that in our asymptotic model, adjacent hexagons are congruent. In particular, $\overrightarrow{AP} = \overrightarrow{EQ}$: the position of Q and R is function of the position of P.

Let us build the lines l_P, l_Q , and l_R where l_P (resp. l_Q, l_R) is the line parallel to (PE) (resp. (QE) and (RE)) passing through N_P (resp. N_Q, N_R). For the structure to be torsion-free, these lines need to be concurrent in a point N_E . The condition $N_E \in l_P$ can be expressed as:

$$N_E = N_P + \lambda \overrightarrow{EP}$$

With λ a real number. Since N_E also belongs to l_Q :

$$\begin{aligned} \overrightarrow{N_Q N_E} \wedge \overrightarrow{Q E} &= 0 \\ (\overrightarrow{N_Q N_P} + \lambda \overrightarrow{EP}) \wedge \overrightarrow{P A} &= 0 \end{aligned}$$

We take the dot product of this quantity with N_P (which is the normal to the plane ACE). We obtain the value of λ as a function of mixed products that depend on the position of P:

$$\lambda = \frac{[N_Q N_P, \overrightarrow{PA}, \overrightarrow{N_P}]}{[\overrightarrow{PE}, \overrightarrow{PA}, \overrightarrow{N_P}]} \quad (2)$$

Finally, N_E also belongs to l_R :

$$\begin{aligned} \overrightarrow{N_R N_E} \wedge \overrightarrow{ER} &= 0 \\ \lambda &= \frac{[N_R N_P, \overrightarrow{PC}, \overrightarrow{N_P}]}{[\overrightarrow{PE}, \overrightarrow{PC}, \overrightarrow{N_P}]} \end{aligned} \quad (3)$$

Combining equations (1) and (2), we obtain the following condition necessarily fulfilled by P for the a point N_E incident to the three lines l_P , l_Q , and l_R to exist:

$$[N_Q N_P, \overrightarrow{PA}, \overrightarrow{N_P}] [\overrightarrow{PE}, \overrightarrow{PC}, \overrightarrow{N_P}] = [N_R N_P, \overrightarrow{PC}, \overrightarrow{N_P}] [\overrightarrow{PE}, \overrightarrow{PA}, \overrightarrow{N_P}]$$

Synthesis

The above equation is a cubic equation in which the only unknown are the coordinates (x, y) of point P. For any given x_0 , we can find at least one solution (x_0, y) in y (a cubic equation of one variable always has at least one root). Doing the reasoning of the “analysis” part upwards, for a solution P of the cubic equation, the lines l_P , l_Q and l_R are concurrent, and the structure is therefore torsion-free.

As a conclusion, the construction showed in Figure 35 is always possible. The hexagonal network (in red) along with the attached normals described by the hexagonal mesh on the Gauss map (also in red) verify all the properties of a Caravel mesh except node repetition (property (d)).

APPENDIX C : ASYMPTOTIC BEHAVIOR OF HEXAGONAL CARAVEL MESHES

In this last appendix, we prove the asymptotic behavior of hexagonal Caravel meshes given in section 5.1.2. Similarly to appendix B, we construct in two steps a geometrical structure that fulfills the Caravel properties at the first order:

Step 1: Construction of a principal PHex mesh

The first step is to construct a PHex mesh aligned with principal curvature directions (Figure 21). In the asymptotic case, each hexagon is then symmetric with respect to the principal curvature directions (Wang and Liu 2009). The Gauss map of the hexagons has the same symmetry.

Step 2: construction of staggered hex grid from Fermat points

Referring to Figure 36, we pick three vertices on a hexagon ABCDEF to form a triangle ACE. We build the Fermat center P of ACE, i.e. the point such that $(\overrightarrow{PA}, \overrightarrow{PC}) = (\overrightarrow{PC}, \overrightarrow{PE}) = (\overrightarrow{PE}, \overrightarrow{PA}) = 120^\circ$. P will be a flat node of the mesh, and A, C and E will be 3D nodes (incident edges at 3D nodes also have 120° angles because of the symmetries). As discussed in the previous section, the node axis at P, N_P , is at the center of the Gauss map of the Dupin indicatrix. It may not coincide with the surface normal at P, n_P . We also build the Fermat points of the adjacent hexagons, Q and R, and their node axes.

We then build on the Gauss map the lines l_P , l_Q and l_R , which are respectively the lines parallel to (PE) , (QE) and (RE) passing through N_P , N_Q and N_R . We observe that, thanks to the symmetry of the Gauss map, the lines l_P , l_Q and l_R are concurrent. The point of concurrency gives the node axis at E, N_E .

The hexagonal network (in red) along with the attached normals described by the hexagonal mesh on the Gauss map (also in red) verify all the Caravel properties and also have a 120° angle between the beam planes of the 3D nodes. We remark that this construction is also valid for surfaces with negative curvature, as illustrated in the right part of Figure 36 (with $k_2 < 0$, so the Gauss map is “inverted” in direction 2). In particular, the process yields convex hexagons, whereas the PHex mesh used as a basis has “bow-tie” shaped hexagons.

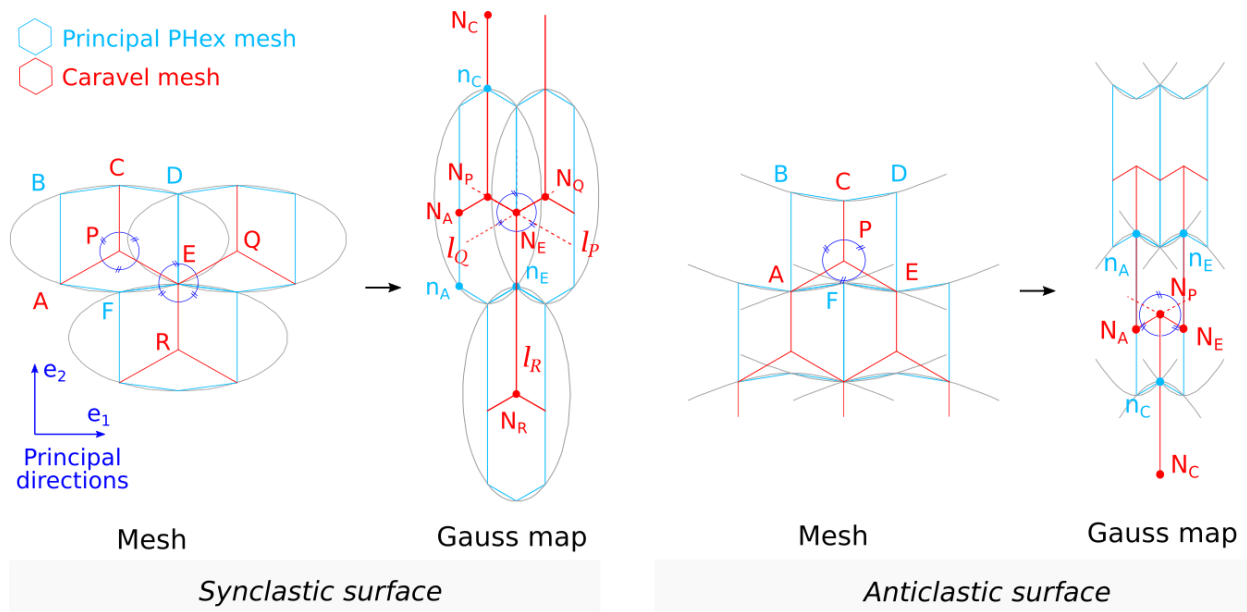


Figure 36: Asymptotic construction of a hexagonal Caravel mesh with 3D nodes at 120°